

# ✓ Dynamic Optimization Of An Industrial Semi-batch Nylon 6 Reactor With Stopping Conditions And End-point Constraints

*A Thesis Submitted in Partial Fulfilment  
of the Requirements for the Degree of*  
MASTER OF TECHNOLOGY

by  
NAVEEN KRISHAN KOHLI

to the

Department of Chemical Engineering  
Indian Institute of Technology, Kanpur  
February, 1996

22 MAR 1996  
CENTRAL LIBRARY  
I.I.T., KANPUR  
Vol. No. A121226

CHE- 1986- M- KCH- DYN



A121226

# CERTIFICATE

This is to certify that the work contained in this thesis, entitled 'DYNAMIC OPTIMIZATION OF AN INDUSTRIAL SEMI-BATCH NYLON 6 REACTOR WITH STOPPING CONDITIONS AND END-POINT CONSTRAINTS' has been carried out by Naveen Krishan Kohli under my supervision and this work has not been submitted elsewhere for a degree.

February, 1996



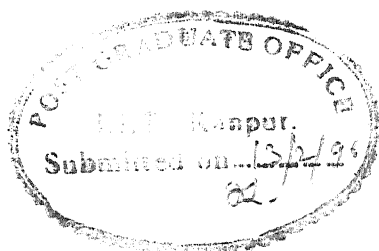
(Santosh K. Gupta)

Professor

Department of Chemical Engineering

Indian Institute Of Technology

Kanpur - 208 016, India



# ACKNOWLEDGEMENT

During my thesis work I have had the pleasure and privilege of interaction with many persons. To adequately acknowledge personally all those who have contributed to make my sojourn (*wish I could stay here for a bit long*) at this place *a memorable* one, would not be possible without risking serious omissions. But it would be ungrateful for me if some persons, without whom this all would not have been possible, are not acknowledged personally.

I would like to thank Prof. S.K.Gupta for guidance, help and freedom he provided to me in achieving, whatever little I could, in this work. From him I have learnt what a TEACHER to a TAUGHT is. Thanx – Sir.

Without Bansal, Gandhi, Verma, Chotu, Sanjay, Chander & Rajiv, the stay at IITK wouldn't have been so colorful and memorable. Thanks are due on Pavitra for being my friend and sharing some intimate moments with me. Thanx – Ritwik, whenever I will think of computers you will be there. I would also like to thank my labmates, Chakri, Sajith, Bhargva, Mankar, Mitra & Palav.

I would like to thank GSFC, Vadodara for partially funding the project. Finally I would like to thank Regional Engineering College, Jalandhar for sponsoring me to this place. I would like to quote a few lines from the thesis of Rajeev Sareen (who stimulated me to the world of Pontryagin's)- "IITK is great place to be. Life is never going to be same again, after leaving IITK."

Naveen Krishan Kohli

# CONTENTS

<u>Item</u>	<u>Page No.</u>
1. Certificate	1
2. Acknowledgement	2
3. List of figures	3
4. List of tables	5
5. Nomenclature	6
6. Abstract	9
7. Introduction	10
8. Formulation	15
9. Results & Discussions	22
10. Conclusions	44
11. Suggestions for future work	45
12. References	46
13. Appendix 1	48
14. Appendix 2	50

# List Of Figures

<u>Figure</u>	<u>Title</u>	<u>Page No.</u>
1	Schematic representation of the industrial semi-batch nylon 6 reactor	12
2	Dimensionless pressure ( $\Pi$ ) histories for the reference (ref) and optimal (opt) runs, for $T_j = T_{j,ref}$ , $[W]_o = 2.52\%$ , $3.45\%$ , $4.43\%$ .	13
3	Starting dimensionless vapor release rate history for $[W]_o = 3.45\%$ (case 2).	23
4	Convergence of dimensionless pressure history with iteration no., for $[W]_o = 3.45\%$ , $\epsilon^* = 0.9$ , $r = 0.1$ (case 2).	24
5	Convergence of objective function, $I (\equiv t_f/t_{f,ref})$ with iteration no. for case 2 (Fig.4).	25
6	$\psi_1 (\equiv conv_{t_f} - conv_d)$ vs. iteration no. for case 2 (Fig.4).	26
7	Dimensionless pressure histories corresponding to three different starting $V_T$ histories, (cases 1-3).	29
8	Dimensionless pressure histories for optimal runs corresponding to three different starting $V_T$ histories (cases 1-3).	31
9	Dimensionless vapor release rate histories. Curve (ref): reference run, (opt): optimal run, for $T_j = T_{j,ref}$ , $[W]_o = 3.45\%$ .	32
10	Dimensionless vapor release rate histories. Curve (ref): reference run, (opt): optimal run, for $T_j = T_{j,ref}$ , $[W]_o = 2.52\%$ .	33
11	Dimensionless vapor release rate histories. Curve (ref): reference run, (opt): optimal run, for $T_j = T_{j,ref}$ , $[W]_o = 4.43\%$ .	34

12	Variation of degree of polymerization with dimensionless time for the reference (ref) and optimal (opt) runs for $T_j = T_{j,ref}$ , $[W]_o = 2.52\%, 3.45\%, 4.43\%$ .	35
13	Variation of dimensionless temperature ( $\theta$ ) with dimensionless time for the reference (ref) and optimal (opt) runs for $T_j = T_{j,ref}$ , $[W]_o = 2.52\%, 3.45\%, 4.43\%$ .	37
14	Variation of the dimensionless monomer conversion with dimensionless time for the reference (ref) and optimal (opt) runs for $T_j = T_{j,ref}$ , $[W]_o = 3.45\%$ (case 2).	38
15	Variation of the dimensionless cyclic dimer concentration with dimensionless time for the reference (ref) and optimal (opt) runs for $T_j = T_{j,ref}$ , $[W]_o = 2.52\%, 3.45\%, 4.43\%$ .	39
16	Optimal pressure history using $T_j = T_{j,ref} + 5^\circ\text{C}$ for the $[W]_o =$ 3.45% case. Optimal history using $T_j = T_{j,ref}$ also shown for comparison.	41
17	Optimal pressure histories for the two optimization problems described in Eqs. 4–6 and Eqs. 15–17 for $[W]_o = 3.45\%$ .	42

## List Of Tables

<u>Table</u>	<u>Title</u>	<u>Page No.</u>
1	Kinetic Scheme for Nylon 6 Polymerization	16
2	Effect Of $r$ and $\epsilon$ On Convergence	28
3	Optimal Conditions for Three Feed Water Concentrations	28



# Nomenclature

$A_i^o, A_i^c$	Frequency factor for $i^{th}$ reaction in absence (o) and in presence (c) of catalytic effect ( $\text{kg mol}^{-1} \text{ hr}^{-1}$ or $\text{kg}^2 \text{ mol}^{-2} \text{ hr}^{-1}$ )
$C_i$	Caprolactam (i=1) and cyclic dimer (i=2)
conv	Monomer conversion (Eq. 7)
DP	Degree of polymerization of polymer product
$E_i^o, E_i^c$	Activation energies for the $i^{th}$ reaction in absence (o) and in presence (c) of catalytic effect (J/mol)
F	Mass of liquid in reactor at time t (kg)
$\Delta H_i$	Enthalpy of the $i^{th}$ reaction (J/mol)
I	Objective function
$I_{\psi_1 I}, I_{\psi_1 \psi_1}, I_{II}$	Integrals of modified adjoint variables
$k_i$	Forward rate constant of $i^{th}$ reaction
$k_i'$	Reverse rate constant of $i^{th}$ reaction
$K_i$	Equilibrium constant for $i^{th}$ reaction
n	Number of equations for state variables
PDI	Polydispersity index
p	Pressure (kPa or atm)
$p_{max}$	Maximum pressure (kPa or atm)
r	Parameters in optimization code
R	Gas constant (J/mol-K)
$R_{V,m}, R_{V,w}$	Rate of vaporization of monomer and water at time t (mol/hr)
S	Slope of p vs t curve in our earlier studies [23,24] (atm/hr)

contd.

$\Delta S_i$	Entropy change for the $i^{th}$ reaction ( $\text{J mol}^{-1} \text{ K}^{-1}$ )
$S_n$	Linear n-mer
$t$	Time (hr)
$t_f$	Total reaction time (hr)
$t_c$	Time for which $p = p_{max}$ (hr)
$T$	Temperature (K)
$T_j$	Jacket fluid temperature (K)
TOL	Tolerance in D02EJF code of NAG library
$\mathbf{u}$	Vector of control variables, $u_i$
$V_T$	Rate of vapor release from reactor (mol/hr)
$W$	Water
$\mathbf{x}$	Vector of state variables, $x_i$

### Greek Letters

$\epsilon^*$	Parameter in optimization code
$\mu_k$	$k^{th}$ moment of the chain length distribution ( $k = 1, 2, \dots$ ) ; $\mu_k \equiv \sum_{n=1}^{\infty} n^k [S_n]$ (mol/kg)
$\mu_n$	Number average chain length ( $\equiv \frac{\mu_1}{\mu_0}$ )
$\Pi$	Dimensionless pressure (Eq. 1)
$\tau$	Dimensionless time (Eq. 2)
$\theta$	Dimensionless temperature
$\zeta_1$	Total moles of monomer vaporized in reactor till time $t$ (mol)
$\omega$	Parameter in Eq. 14

contd.

$\rho$	Stopping condition
$\psi_1$	End-point constraint
$\lambda_i$	Adjoint variables
$\lambda_i^{I\rho}, \lambda_i^{\psi_1\rho}$	Modified adjoint variables

### Subscripts/Superscripts

d	Desired value
f	Final (value for the product)
j	jacket
max	Maximum value
o	Feed conditions
$t_f$	Value at $t=t_f$
ref	Reference (value used in industrial reactor currently)

### Symbols

[ ]	Concentrations (mol/kg mixture)
-----	---------------------------------

# ABSTRACT

In this study, optimal vapor release rate (or pressure) histories have been generated for an industrial semi-batch nylon 6 reactor using Pontryagin's minimum principle. The batch time has been taken as the objective function, which is to be minimized. The pressure is constrained to lie between a lower and an upper limit. The temperature, a state variable, is also constrained to lie between 220° C and 270° C in order to ensure single-phase polymerization. Optimization has been carried out with a single end-point constraint (on monomer conversion) and a stopping condition (obtaining a product having a desired degree of polymerization,  $\mu_n$ ). Techniques have been developed to overcome the discontinuities present in the model, as well as to take care of state variable constraints. The effects of various physical and computational variables on the optimal pressure history and the corresponding batch time have been studied. It is found that the optimal batch time is almost 50% of the industrial value used currently. Interestingly, the optimal pressure history is quite similar *qualitatively* with the current practice though *quantitatively* there is a significant difference. Improvements in reactor operation along these lines have been reported.

# Introduction

A significant amount of research on the simulation of nylon 6 polymerization has been reported in the past few years. These have formed the subject of several reviews [1-5]. The effects of various operating variables (initial water concentration, temperature, monofunctional acid stabilizers, initial monomer concentration, etc.) on the characteristics of the product [viz., monomer conversion, degree of polymerization (DP or  $\mu_n$ ), polydispersity index (PDI), etc.] are now well established. The early reports have been followed by several studies [6-16] on the optimization of nylon 6 reactors. Hoftyzer et al. [6] used dynamic programming to determine the optimal temperature and water concentration (related to total applied pressure) histories,  $T(t)$  and  $[W](t)$ , required for producing nylon 6 having a desired value,  $\mu_{n,d}$ , of the degree of polymerization in the shortest possible reaction time,  $t_f$ . Unfortunately, Hoftyzer et al. presented only semiquantitative results, because of proprietary reasons. Reimschuessel and Nagasubramanian [7,8] optimized combinations of two-stage isothermal reactors, and presented quantitative results. These two studies made use of a kinetic scheme involving only the major reactions (ring opening, polycondensation, and polyaddition). Naudin ten Cate [9] and Mochizuki and Ito [10] used the minimum principle to find optimal temperature profiles in tubular reactors. Naudin ten Cate optimized a two stage reactor, the first one at temperature  $T_o$ , having a residence time  $t_o$ , in which water is vaporized continuously. This was followed by a nonvaporizing tubular reactor having a residence time  $t_f - t_o$ . Mochizuki and Ito, however, optimized a single reactor. Both these groups of workers used semiempirical approximations for the rates of formation of the undesirable cyclic oligomers, and attempted to minimize the formation of the water extractable compounds (cyclic oligomers, water and unreacted monomer) while simultaneously keeping some product characteristics fixed (end-point constraints). These

workers assumed no evaporation of water and/or caprolactam and obtained optimal temperature histories. Again, only semiquantitative results were presented. Dynamic optimization of batch (or tubular) reactors using a variety of objective functions and end-point constraints has been carried out by our group [11-16] using Pontryagin's minimum principle [17,18]. These studies have shown that the optimal histories are largely dependent, both qualitatively and quantitatively, on the choice of the objective function and the constraints. This observation is consistent with similar observations made by Ray and Szekely [17] and Denn [18], who have compiled the results of several optimization studies for nonpolymeric systems. Most of these studies give valuable insight into the optimal operation of *ideal* reactors, and indeed, these must have been used in the design and improvement of nylon 6 reactors in industry over the years. Work on the modelling of actual *industrial* reactors has only just started to appear in the open literature [19]. In this study, the operation of one such reactor (semi-batch nylon 6 reactor) has been optimized using Pontryagin's minimum principle [17,18,20,21]. Optimal pressure histories have been obtained for the manufacture of three grades of polymer. Substantial improvements are possible in the performance of this reactor once these are implemented.

The industrial reactor studied here is shown schematically in Fig.1. It is a jacketed vessel with a low speed anchor or ribbon agitator used for mixing the highly viscous reaction mass. The reaction mass (caprolactam, water and other inert additives like  $\text{TiO}_2$ , etc.) is heated by condensing vapors in a jacket. As the polymerization takes place the temperature inside the reactor goes above  $220^\circ\text{C}$  and vaporization of caprolactam and water takes place, resulting in build up of pressure. The pressure inside the reactor,  $p(t)$ , is maintained to conform to a desired history by manipulation of a control valve which allows the vapor mixture of nitrogen, monomer and water to pass to a condenser. The pressure histories used currently (referred to as 'reference' conditions) for three different industrial runs producing different grades of nylon

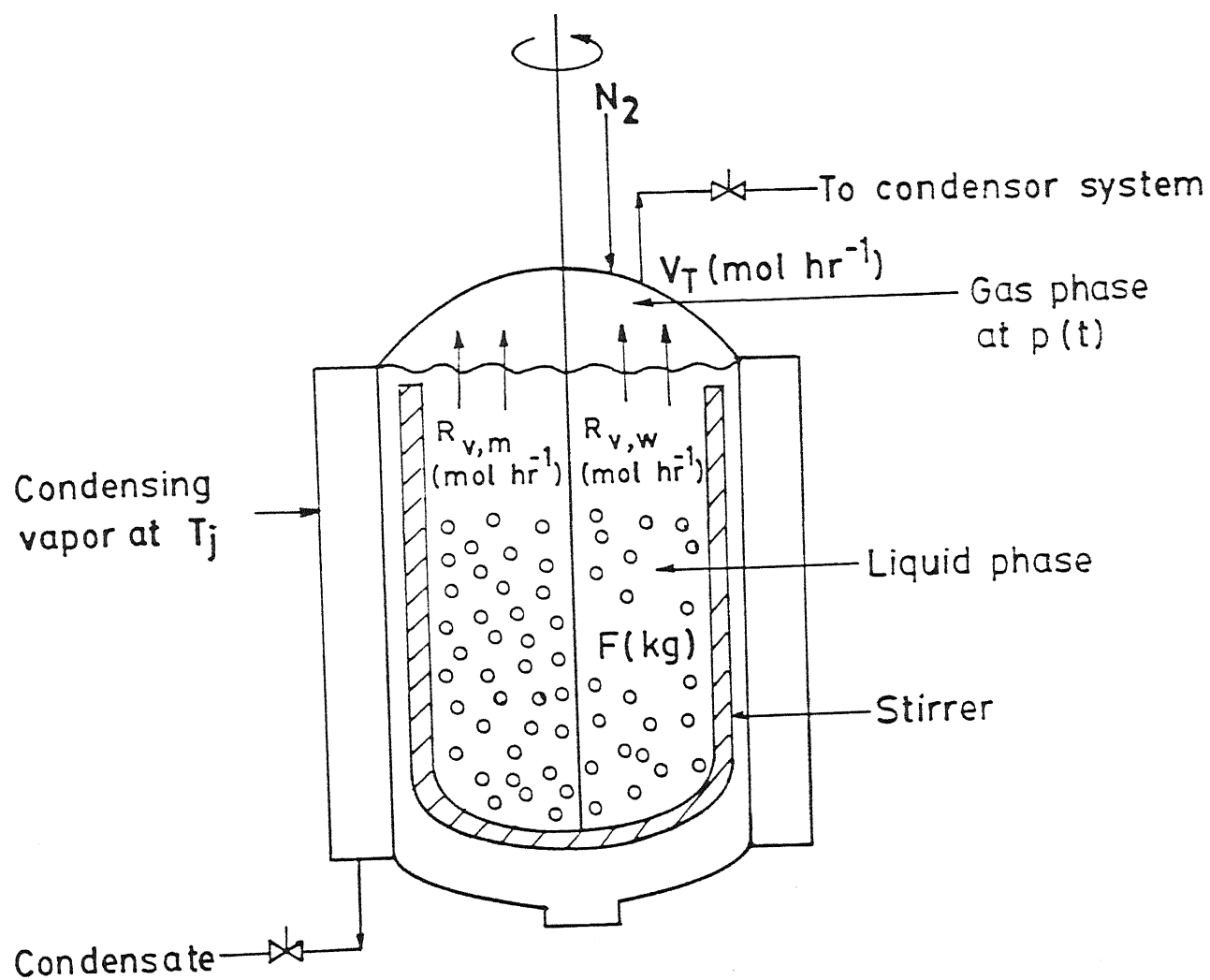


Fig.1 Schematic representation of the industrial semi-batch nylon 6 reactor

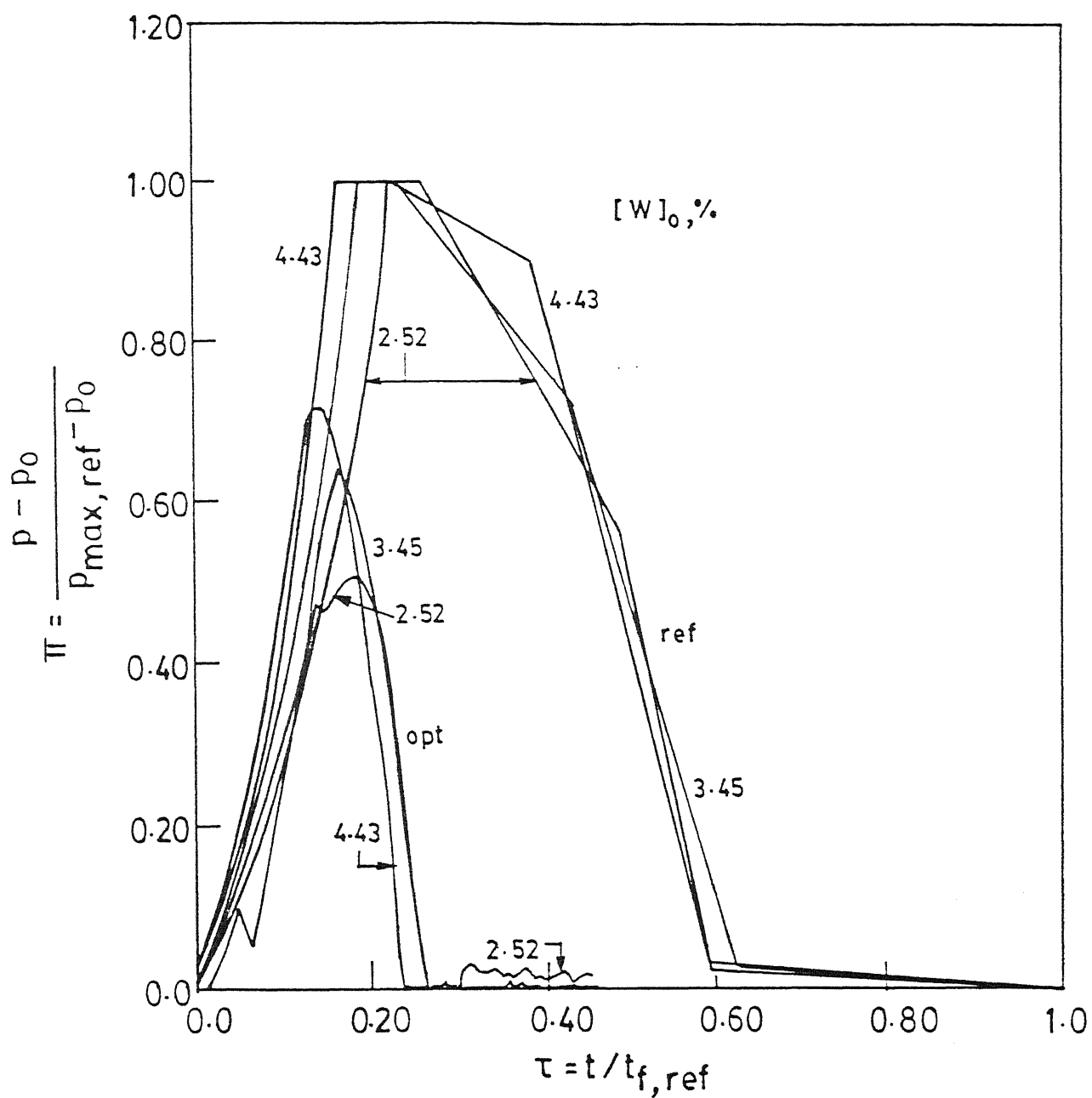


Fig.2 Dimensionless pressure ( $\Pi$ ) histories for the reference (ref) and optimal (opt) runs, for  $T_j = T_{j,ref}$ ,  $[W]_0 = 2.52\%$ ,  $3.45\%$ ,  $4.43\%$ .



6, are shown in Fig.2 (curves marked ‘ref’). In this figure, the pressure and the reaction time,  $t$ , have been nondimensionalized using [19] (see nomenclature)

$$\Pi \equiv (p - p_o)/(p_{max,ref} - p_o) \quad (1)$$

$$\tau \equiv t/t_{f,ref} \quad (2)$$

The values of the maximum pressure,  $p_{max,ref}$ , and the total reaction time,  $t_{f,ref}$ , used currently, are not being reported for proprietary reasons. The jacket temperature,  $T_j$ , is kept constant throughout the reaction at the current value,  $T_{j,ref}$ .

## CHAPTER 2

# FORMULATION

The kinetic scheme for nylon 6 polymerization is given in Table 1 [4]. This kinetic scheme incorporates the three important reactions *viz.* ring opening, polycondensation and polyaddition, as well as reactions with the cyclic dimer. Because of the unavailability of precise information about the rates of the reactions involving higher cyclic oligomers, these have not been incorporated in Table 1. Since the cyclic dimer constitutes a major share of the total cyclic oligomers in the reaction mass, this assumption is justified. The equations for the fifteen state variables,  $x_i$  (mass and energy balance, and moment equations) are given in appendix 1 [19]. In general the state variable equations can be expressed as:

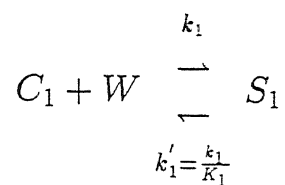
$$\frac{dx_i}{dt} = f_i(\mathbf{x}, \mathbf{u}); i = 1, 2, \dots, 15 \quad (3)$$

where  $\mathbf{x}$  and  $\mathbf{u}$  are the vectors of the state and control variables.

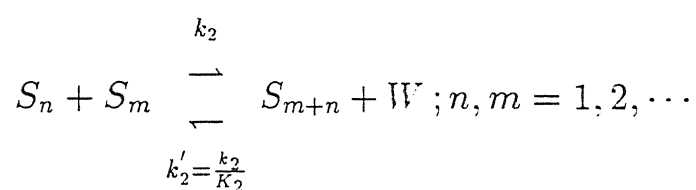
The ODEs (ordinary differential equations) in Eq.3 can be integrated using the D02EJF subroutine of the NAG library. This uses Gear's technique for integrating sets of stiff ODEs [22]. The presence of some discontinuities and the stiffness of ODEs make it difficult to use a constant error tolerance (TOL) in the computer code. Provision was made in the algorithm for self-adjustment of the error tolerance between  $10^{-4}$  and  $10^{-12}$ . When D02EJF failed to solve the ODEs with the given error tolerance, it came out of the subroutine giving an error message, IFAIL=2. At this point a backward step was taken and TOL reduced by a factor of 10. The ODEs were again integrated in the forward direction. This backward movement was continued with a reduction in TOL, and the integration repeated till the solution was obtained. A similar procedure was followed for the backward integration of the adjoint variables. The change in viscosity of the reaction mixture and its effect on the mass transfer rates have been incorporated

Table 1  
KINETIC SCHEME FOR NYLON 6 POLYMERIZATION

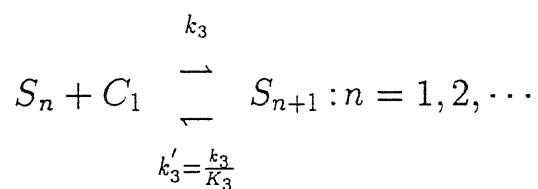
1. Ring Opening



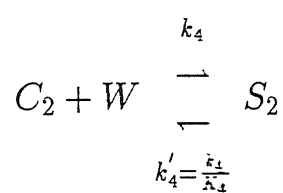
2. Polycondensation



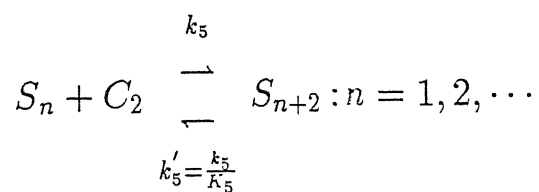
3. Polyaddition



4. Ring Opening Of Cyclic Dimer



5. Polyaddition Of Cyclic Dimer



contd....

## Rate and Equilibrium Constants

$$\begin{aligned}
 k_i &= A_i^o \exp(-E_i^o/RT) + A_i^c \exp(-E_i^c/RT) \sum_{n=1}^{\infty} ([S_n]) \\
 &= k_i^o + k_i^c \sum_{n=1}^{\infty} ([S_n]) \\
 K_i &= \exp [(\Delta S_i - \Delta H_i/T)/R] , i = 1, 2, \dots, 5
 \end{aligned}$$

$i$	$A_i^o$ (kg/mol-h)	$E_i^o$ (cal/mol)	$A_i^c$ (kg <sup>2</sup> /mol <sup>2</sup> -h)	$E_i^c$ (cal/mol)	$\Delta H_i$ (cal/mol)	$\Delta S_i$ (cal/mol-K)
1	$5.9874 \times 10^5$	$1.9880 \times 10^4$	$4.3075 \times 10^7$	$1.8806 \times 10^4$	$+1.9180 \times 10^3$	$-7.88460$
2	$1.8942 \times 10^{10}$	$2.3271 \times 10^4$	$1.2114 \times 10^{10}$	$2.0670 \times 10^4$	$-5.9458 \times 10^3$	$+0.94374$
3	$2.8558 \times 10^9$	$2.2845 \times 10^4$	$1.6377 \times 10^{10}$	$2.0107 \times 10^4$	$-4.0438 \times 10^3$	$-6.94570$
4	$8.5778 \times 10^{11}$	$4.2000 \times 10^4$	$2.3307 \times 10^{12}$	$3.7400 \times 10^4$	$-9.6000 \times 10^3$	$-14.5200$
5	$2.5701 \times 10^8$	$2.1300 \times 10^4$	$3.0110 \times 10^9$	$2.0400 \times 10^4$	$-3.1691 \times 10^3$	$+0.58265$

[19] using correlations for the viscosity of the reaction mass and the activity coefficients of water and caprolactam (see appendix 1). These correlations have been developed [19] by curve-fitting one set of industrial data, and have been found to be satisfactory for other operating conditions.

The simulation package can be used to predict several important properties of the product ( $\mu_n$ , PDI, monomer concentration, cyclic dimer concentration, etc.) as well as the various reactor characteristics [heat and mass transfer coefficient, vapor discharge rate,  $V_T(t)$ , temperature, etc.]. The model of the industrial semi-batch nylon 6 reactor can be used to optimize its operation. In this study, we obtain the optimal vapor-release-rate history,  $V_T(t)$ , which minimizes the total reaction time,  $t_f$ , while requiring a few constraints to be met at  $t=t_f$ . The objective function,  $I$ , to be minimized is selected as the dimensionless total reaction time

$$\min I [\mathbf{x}(t), t_f] \equiv t_f/t_{f,ref} \quad (4)$$

where  $t_{f,ref}$  is the total reaction time being used in the reference case (current value). We choose the following constraint at the end point:

$$\psi_1 \equiv conv_{t_f} - conv_d = 0 \quad (5)$$

where the monomer conversion,  $conv$ , at the end of the reaction is forced to be equal to a desired value,  $conv_d$ , selected as the current value. This ensures no additional load on downstream extraction units. In addition, we use the following stopping condition:

$$\rho \equiv \mu_{n,t_f} - \mu_{n,d} = 0 \quad (6)$$

where the number average chain length of the product,  $\mu_{n,t_f}$ , is forced to be equal to a desired (current) value,  $\mu_{n,d}$ . In Eqs.4-6, we have (see nomenclature)

$$conv = 1 - \frac{F[C_1] + \zeta_1}{F_o[C_1]_o} \quad (7)$$

$$\mu_n = \mu_1/\mu_o \quad (8)$$

The stopping condition on  $\mu_n$  ensures the required quality and physical properties of the product (the stopping condition and the end point constraints are interchangeable – in fact, if there are several requirements at  $t=t_f$ , any one can be selected as the stopping condition).

The problem defined in Eqs.4–6 involves three important characteristics of nylon 6 reactors : monomer conversion,  $\mu_n$  and reaction time. One would also like to minimize the cyclic dimer concentration,  $[C_2]_{t_f}$  in the product, *simultaneously*. This, however, would lead to a dynamic multiobjective optimization problem, involving the generation of a Pareto set [16,23]. Such a problem is associated with severe computational problems for the semibatch reactor studied here, and one must have a good knowledge of solutions of simpler optimization problems before one can hope to solve for the Pareto sets. It is hoped that the simpler problem defined in Eqs.4-6 will lead to sufficiently low values of  $[C_2]_{t_f}$  (compared to values encountered currently) and will be satisfactory as well as useful for industrial implementation.

The algorithm for the *general* optimization problem (with one stopping and  $m$  end-point constraints as well as  $n$  state variable equations and  $l$  control variables) [14] is given in appendix 2. In the present case, three sets of adjoint variables,  $\lambda_i^I$ ,  $\lambda_i^{\psi_1}$  and  $\lambda_i^o$  ( $i = 1, 2, \dots, n$ ) have to be evaluated. The ODEs defining these variables are similar in form but their values differ because of the different boundary conditions at  $t=t_f$ . The numerical procedure used is as follows [14]:

1. An initial control variable history (a single control variable,  $u \equiv V_T$ , is used in this study),  $V_T^o(t)$ , is selected. In order to reduce the memory storage requirements, the values of  $V_T^o$ , and the  $\lambda$ 's are stored at intervals of 0.1 hr and linear interpolation used. The 15 state variable equations with known initial values,  $x(0)$ , are then integrated in the forward direction, using the D02EJF subroutine of the NAG library. The forward integration is carried out until the stopping condition of Eq. 6 is satisfied within some tolerance limit ( $10^{-2}$  in this study). This fixes the value of  $t_f$ . During the forward integration, the values

of  $\partial f / \partial V_T$  and  $\partial f / \partial \mathbf{x}$  [14] are also computed (numerically) and stored at time intervals of 0.1 hr.

2. The adjoint variable equations are then integrated in the backward direction until  $t=0$ , using the D02EJF subroutine, and the boundary conditions at  $t=t_f$ . The modified adjoint variables,  $\lambda_i^{I\rho}(t)$  and  $\lambda_i^{\psi_1\rho}(t)$ , are computed at each storage location ( $\Delta t=0.1$  hr). In addition, the three integrals,  $I_{\Psi_1\Psi_1}$ ,  $I_{\Psi_1 I}$  and  $I_{II}$ , are computed using the D01GAF subroutine of the NAG library.
3. Values of two computational parameters,  $r$  and  $\epsilon^*$  [14], are selected, and the correction,  $\delta V_T$ , computed at each storage location. The new vapor-release-rate history,  $V_T^{new}$ , is generated using:

$$V_T^{new}(t) = V_T^o(t) + \delta V_T(t) \quad (9)$$

4. This completes one iteration. These steps may be repeated (using the new  $V_T$  history as  $V_T^o$ ) until there is no change in the pressure (or  $V_T$ ) history and the end-point constraints are satisfied to a prescribed degree of accuracy (because first order techniques converge very slowly as the optimum is reached).

While carrying out the optimization, it was desired to constrain some of the state variables to lie between lower and upper bounds:

$$0 \leq \Pi \leq 1.0 \quad (10)$$

$$220^\circ C \leq T \leq 270^\circ C \quad (11)$$

The upper bound on pressure does not allow the pressure rating of the industrial reactor to be exceeded while the lower bound ensures the pressure inside to be above atmospheric. The lower limit on  $T$  is the melting point of nylon 6 while the upper limit represents the approximate

boiling point of pure caprolactam (at atmospheric pressures). A standard procedure of satisfying these constraints on the state variables, is to incorporate them into the objective function as penalty functions. Our previous experience (initial runs) has shown that the temperature in the reactor almost never violates the constraints. Therefore, the only state variable for which constraints need to be taken care of, is the pressure inside the reactor. This is controlled by the vapor discharge rate,  $V_T$ , from the reactor. This suggests an empirical (and easier) approach to satisfy the constraints on  $p(t)$  in Eq.10. Some conditional statements have been included in the computer code, which take care of the pressure going below or above the lower and upper values, respectively. Whenever the pressure drops below  $p_o$ ,  $V_T$  is decreased in infinitesimally small steps till the lower bound is satisfied. In a similar way, the upper bound in Eq.10 is taken care of. The computer code so developed was found to work satisfactorily. The correctness of the code was checked by running it for some special cases. The program was run in the simulation mode, using  $V_T(t)$  from Ref. 19. The results were in complete agreement with the earlier simulation results, thereby suggesting that at least in the simulation subroutine, there were no errors. Hand calculations were also performed using the Euler method [22] and some of the adjoint variables computed. These matched values generated by the code. These checks suggest that the code is relatively free of errors. The optimization code took a CPU time of about 1hr 51min on a DEC 3000  $\alpha$ xp machine (for about 450 iterations).



# RESULTS AND DISCUSSIONS

The reference (current operating conditions indicated by 'ref') results are first generated using the simulation code [19] for the three initial water concentrations,  $[W]_o$ , of 3.45%, 2.52% and 4.43% (by weight). The values of several variables describing the current operating conditions are given in Refs. 19 and 23. These provide values of  $\text{conv}_d$  and  $\mu_{n,d}$  in Eqs.5 and 6, and also provide results against which optimal solutions can be compared. The current (ref) pressure histories for the three values of  $[W]_o$  are shown in Fig.2.

Optimal  $V_T(t)$  histories are now generated (with  $T_j = T_{j,ref}$ ), using the following parameters in the algorithm (see appendix 2)

$$r = 0.1 \tag{12}$$

$$\epsilon^* = 0.9 \tag{13}$$

The starting control variable history,  $V^o_T$ , is shown in Fig.3 (case 2). This is selected so as to give the starting pressure history shown as Iteration no. 1 in Fig.4. The pressure builds up to a maximum value,  $p_{max}$  ( $\leq p_{max,ref}$ ) in the beginning, is then maintained at this value for some period of time, and then decreases slowly to the final value at  $t=t_f$  (determined by the stopping condition in Eq. 6). Fig.4 shows the variation of the pressure history with iteration number during the course of optimization for the  $[W]_o = 3.45\%$  case. The objective function, end point constraint violation, and the pressure history converge (see Figs.4-6) to near optimal values in about 332 iterations. In the initial phase of optimization, the convergence is observed to be very rapid but then it slows down and some oscillatory behaviour is observed before final convergence. This kind of oscillatory behaviour has been observed in earlier studies [12-14] also. The convergence of the algorithm can be expedited by manipulating the two

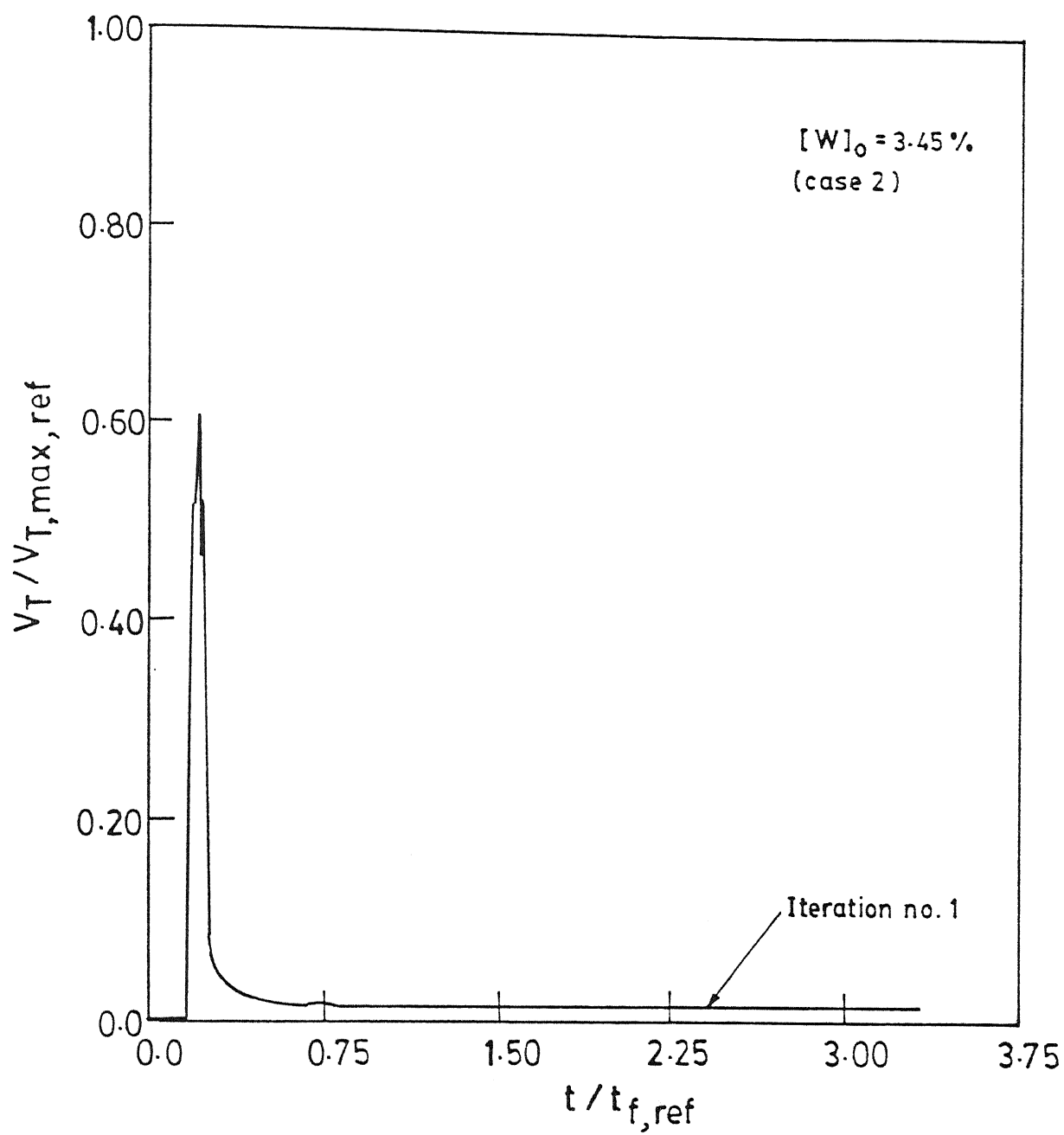


Fig.3 Starting dimensionless vapor release rate history for  $[W]_0 = 3.45\%$  (case 2).

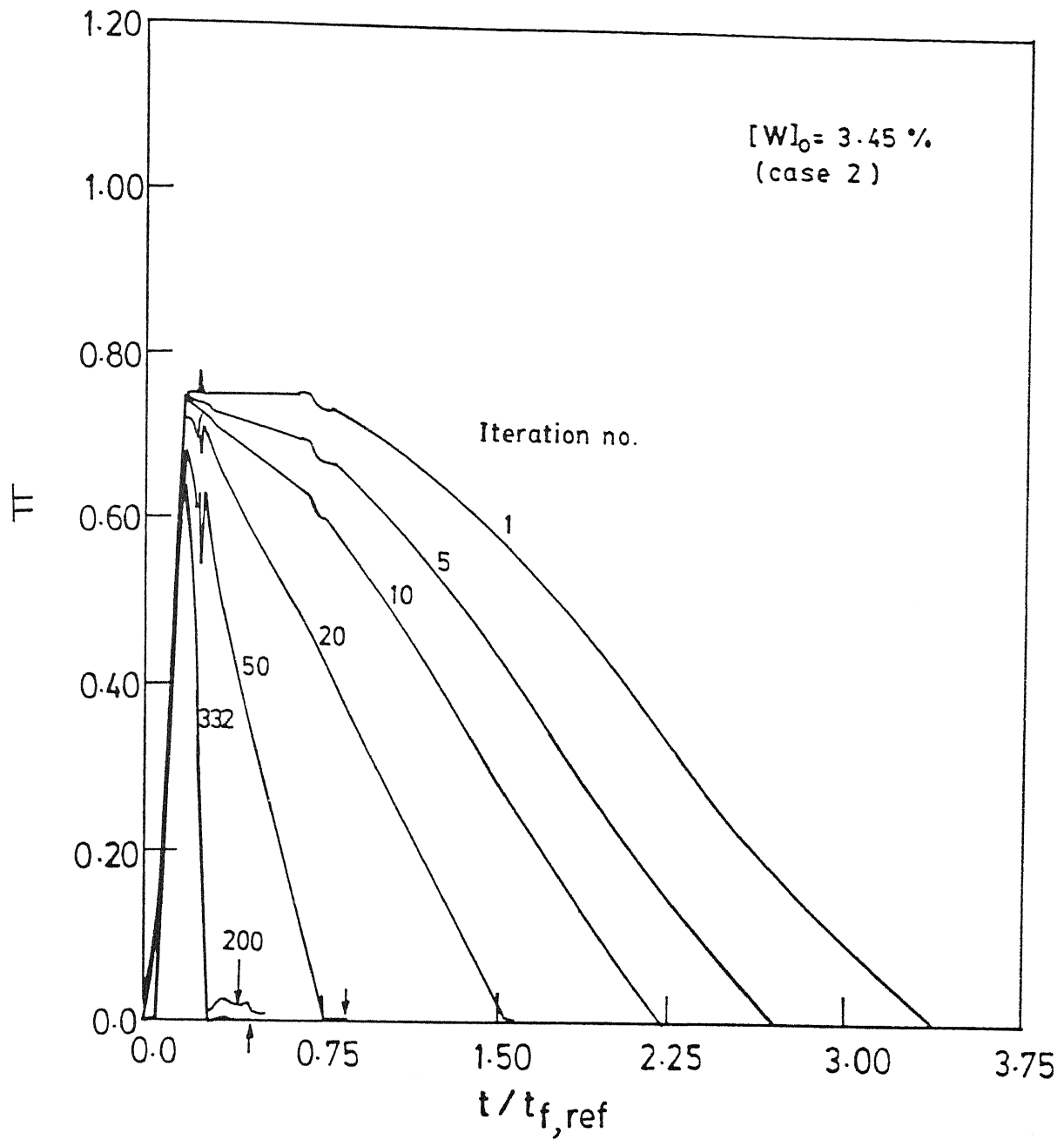


Fig.4 Convergence of dimensionless pressure history with iteration no., for  $[W]_0 = 3.45\%$ .  $\epsilon^* = 0.9$ ,  $r = 0.1$  (case 2).

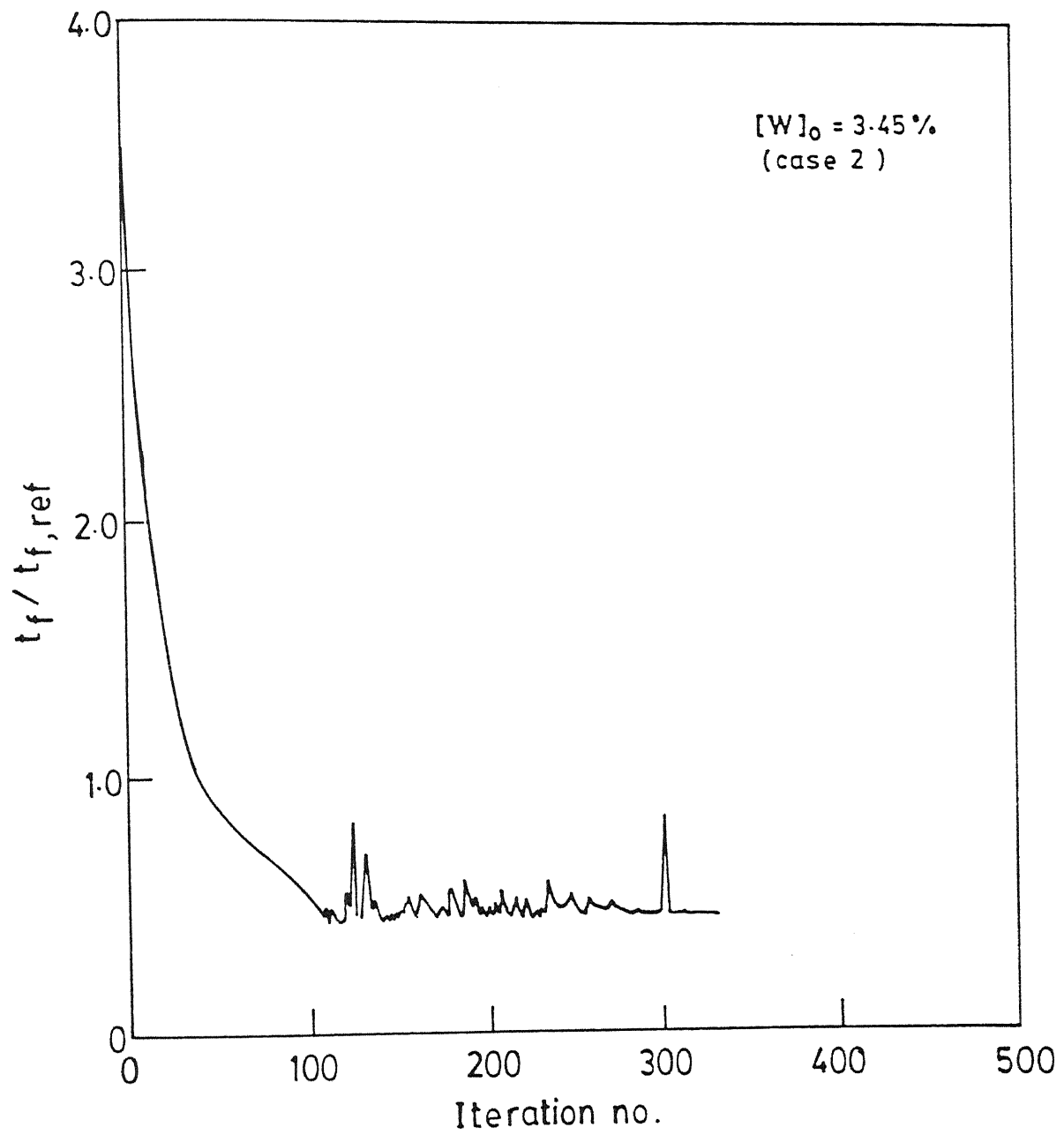


Fig.5 Convergence of objective function,  $I (\equiv t_f/t_{f,ref})$  with iteration no. for case 2 (Fig.4).

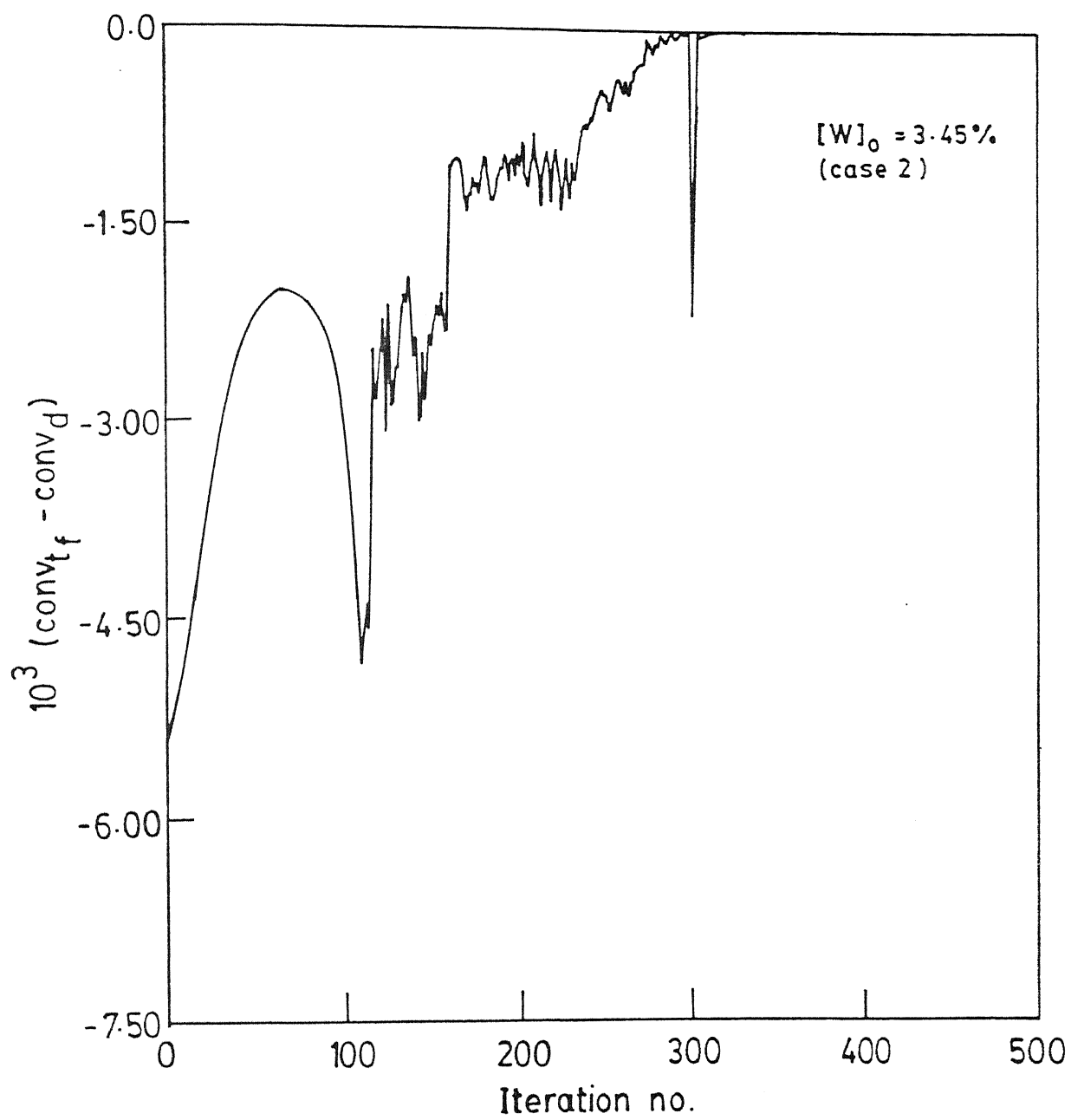


Fig.6  $\psi_1(\equiv conv_{t_f} - conv_d)$  vs. iteration no. for case 2 (Fig.4).

computational parameters,  $\varepsilon^*$  and  $r$ . In the earlier studies [13,14] it has been established that higher values of  $\varepsilon^*$  tend to speed up convergence. But all our attempts to do so were thwarted by the presence of discontinuities in the model. A large value of  $\varepsilon^*$  results in large values of  $\delta\psi_1$ , which lead to large changes in the control vector,  $V_T(t)$ . This results in a sudden drop of pressure. The pressure could go down to such an extent that sudden changes in the interfacial concentrations of monomer and water are observed. The gradient of the monomer concentration (at the bubble surface) then becomes negative. This creates problems in the integration of the state-variable equations, since mass transfer from the bubble to the liquid is not allowed for in the model (and probably does not occur). To avoid such numerical problems, the value of the increment,  $\delta V(t)$ , is modulated by a factor  $\omega (\leq 1)$ . In this study the value of  $\omega$  has been used as 0.75. Therefore, Eq.9 is replaced by

$$V_T^{new}(t) = V_T^o(t) + \omega \delta V_T(t) \quad (14)$$

in the algorithm.

One of the most crucial parameters in the control vector optimization technique [17] is the choice of the initial control vector history,  $V_T^o(t)$ . An improper choice of the initial guess can lead to erroneous results or lack of convergence. A common practice followed in most studies has been to assume a constant value of the control variable at all values of  $t$ . In our study, it was not possible to start with such a history since it led to negative gradients of the monomer concentration at the bubble surface. Therefore, a  $V_T^o$  history was selected which corresponded to an initial pressure history,  $p^o(t)$ , which was somewhat similar to the one being used currently in the industrial reactor (see Fig.2). Optimization was carried out with three different initial  $V_T^o$  histories (cases 1–3). Fig.7 shows the initial (Iteration No. 1) pressure histories for these three cases. The optimal history is found to be almost independent of the starting history (see Fig. 8), and the values of  $t_f/t_{f,ref}$  ( $=0.45$ ) match to two decimal places. Optimization

Table 2  
Effect Of  $r$  and  $\epsilon^*$  On Convergence<sup>+</sup>  
[W]<sub>o</sub> = 3.45% (Case 2)

$\epsilon^*$	$r$	Iterations	CPU Time (sec)
0.75	0.50	374	6734
0.90*	0.10	332	6182
0.50	0.05	455	7088
0.50	0.10	455	6628
0.50	0.25	455	7015
0.50	0.50	455	6946
0.50	1.00	455	7023

+  $t_f/t_{f,ref} = 0.45$ ;  $conv_{t_f}/conv_d = 1.00$  for all cases

\* *bestvalue*

Table 3  
Optimal Conditions for Three Feed Water Concentrations

[W] <sub>o</sub> %	$t_f/t_{f,ref}$	$conv_{t_f}/conv_d$	$[C_2]_{t_f}/[C_2]_{t_f,ref}$
2.52	0.43125	0.99956	0.2526559
3.45	0.45000	1.00000	0.2584115
4.43	0.46250	0.99977	0.2491274

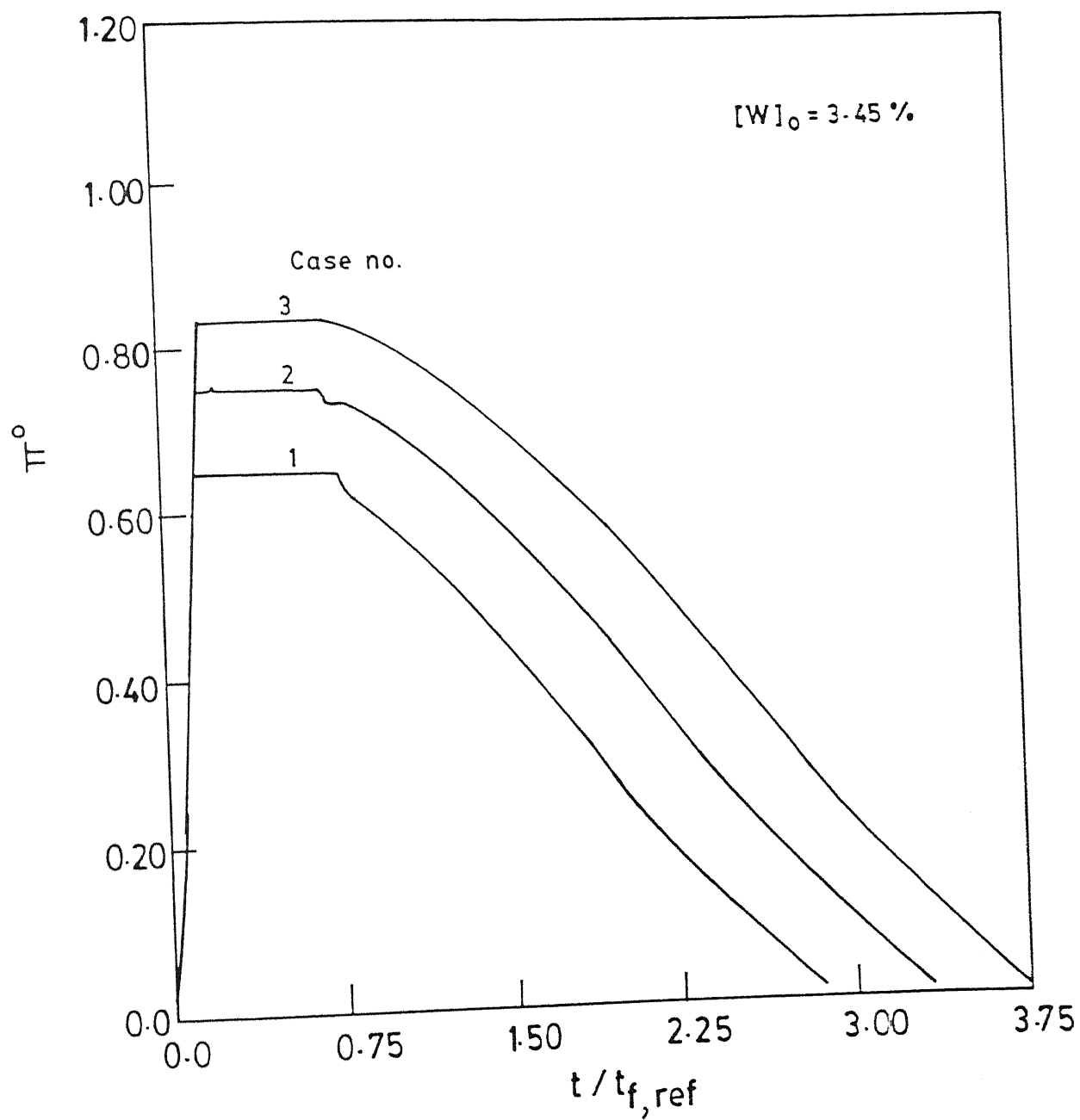


Fig.7 Dimensionless pressure histories corresponding to three different starting  $V_T$  histories, (cases 1-3).



has also been carried out with different combinations of  $\epsilon^*$  and  $r$ . Table 2 gives the results. It can be inferred that the final results are independent of the values of the computational parameters (provided that the choices are such that negative monomer concentration gradients at the bubble surface are not encountered). It is found that increasing the value of  $\epsilon^*$  leads to faster convergence (but for certain combinations of the computational parameters, a higher value of  $\epsilon^*$  leads to erroneous results and oscillatory behaviour). Although the value of  $r$  does not affect the number of iterations too much, it has some effect on the CPU time and the amount of oscillatory behaviour. Higher oscillations result in a sudden rise in the objective function which implies more number of calculations in the forward and backward integration steps, thereby resulting in higher CPU times. Thus, some amount of numerical experimentation has to be performed before the best choices of  $r$  and  $\epsilon^*$  can be deduced. We recommend use of values of 0.9 and 0.1 for  $\epsilon^*$  and  $r$  (Eq. 12 and 13), respectively, for the present study.

Fig.2 shows the optimal pressure histories (curves marked 'opt') for the three values of  $[W]_o$ . The plot for  $[W]_o=3.45\%$  is the same as in Figs.4 and 8. The current and optimal vapor release rates are shown in Figs.9–11. Two different maxima in the current  $V_T$  histories are observed. The first maximum corresponds to the opening of the valve for the first time to arrest the increase in pressure associated with early vaporization, while the later one is associated with the desired rapid fall of the pressure. It is evident from Figs.9–11 that different pressure histories and vapor release rates are required to produce three different grades of polymer. Table 3 gives the optimal conditions for the three water concentrations.

Fig.12 shows the variation of  $\mu_n$  with  $t$  for the optimal as well as the reference runs for the three  $[W]_o$  values. In the reference (current) runs, two distinct regions are observed where  $\mu_n$  increases, the first being associated with the polyaddition reaction while the second with the polycondensation reaction. There is a short plateau in-between the two regimes. From the

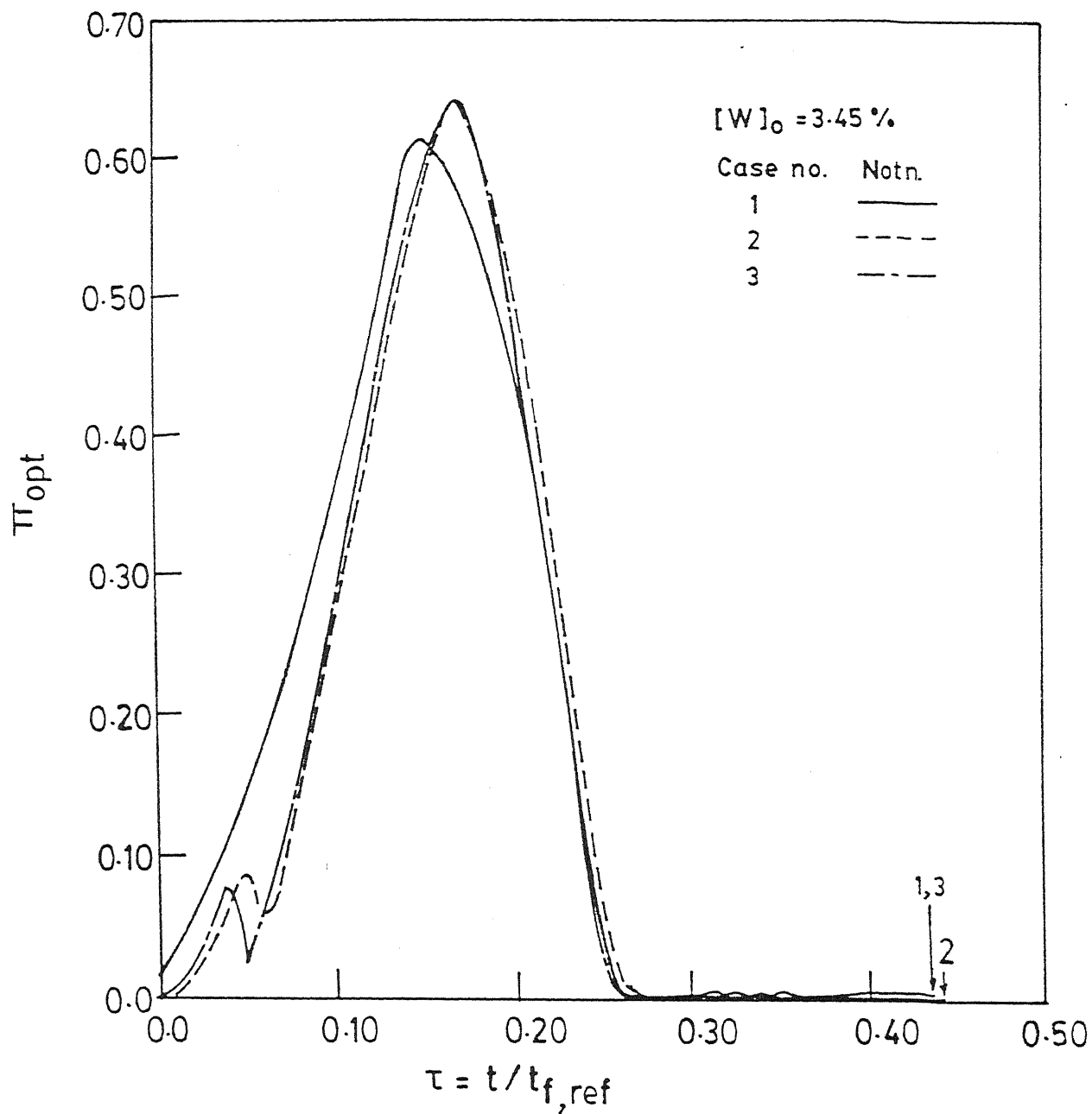


Fig.8 Dimensionless pressure histories for optimal runs corresponding to three different starting  $V_T$  histories (cases 1-3).

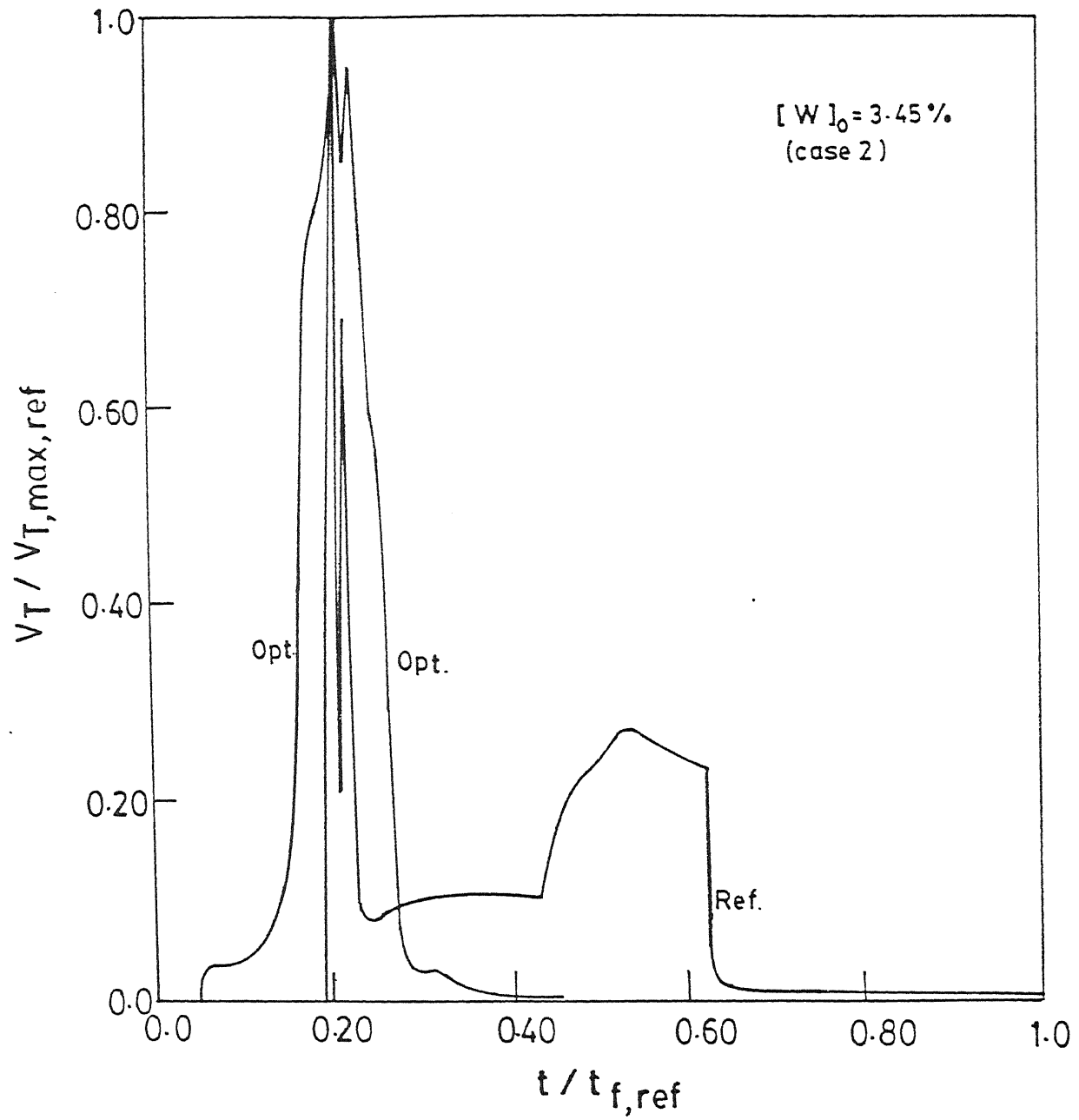


Fig.9 Dimensionless vapor release rate histories. Curve (ref): reference run, (opt): optimal run, for  $T_j = T_{j,ref}$ ,  $[W]_0 = 3.45\%$ .

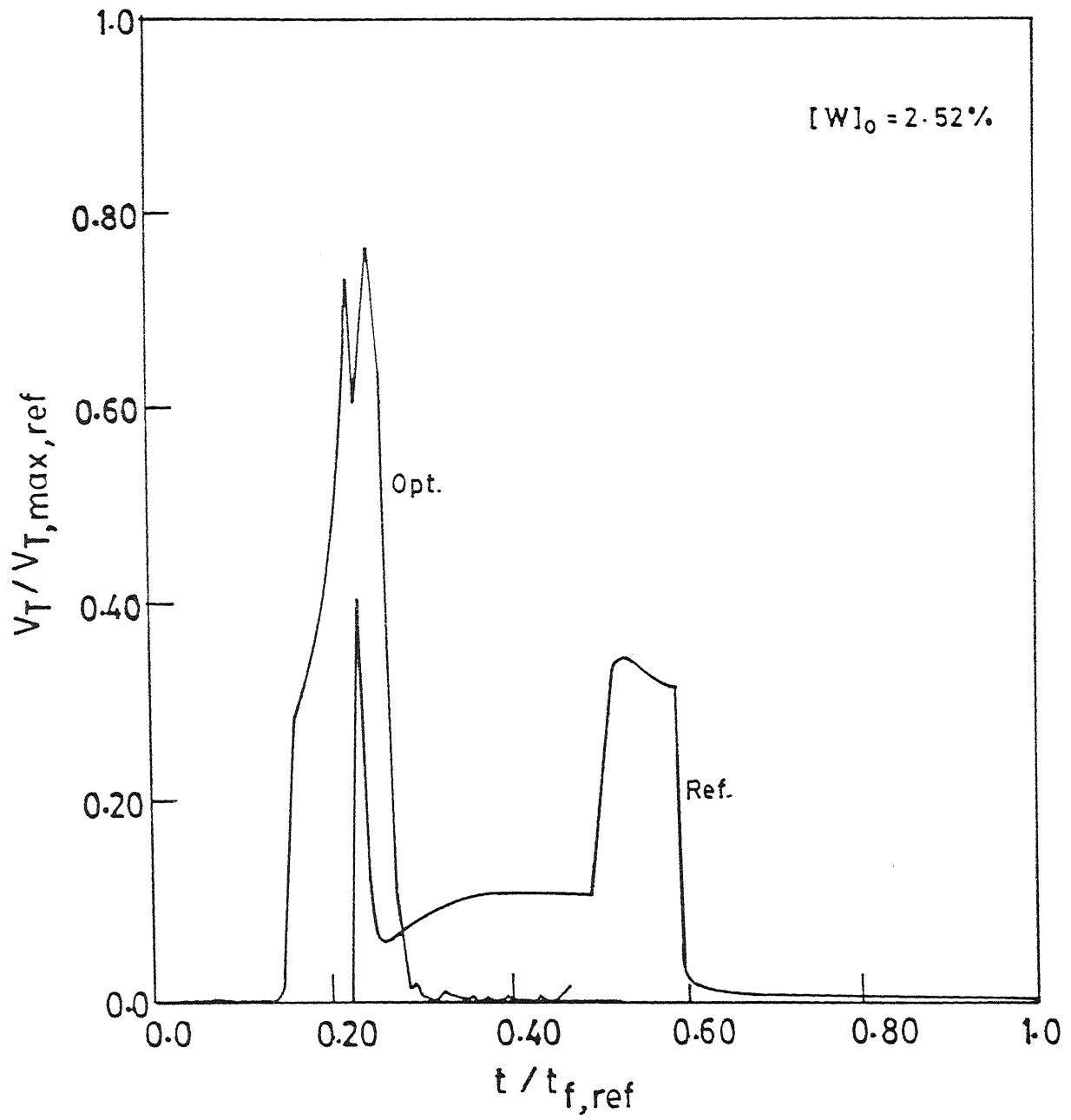


Fig.10 Dimensionless vapor release rate histories. Curve (ref): reference run, (opt): optimal run, for  $T_j = T_{j,ref}$ ,  $[W]_0 = 2.52\%$ .

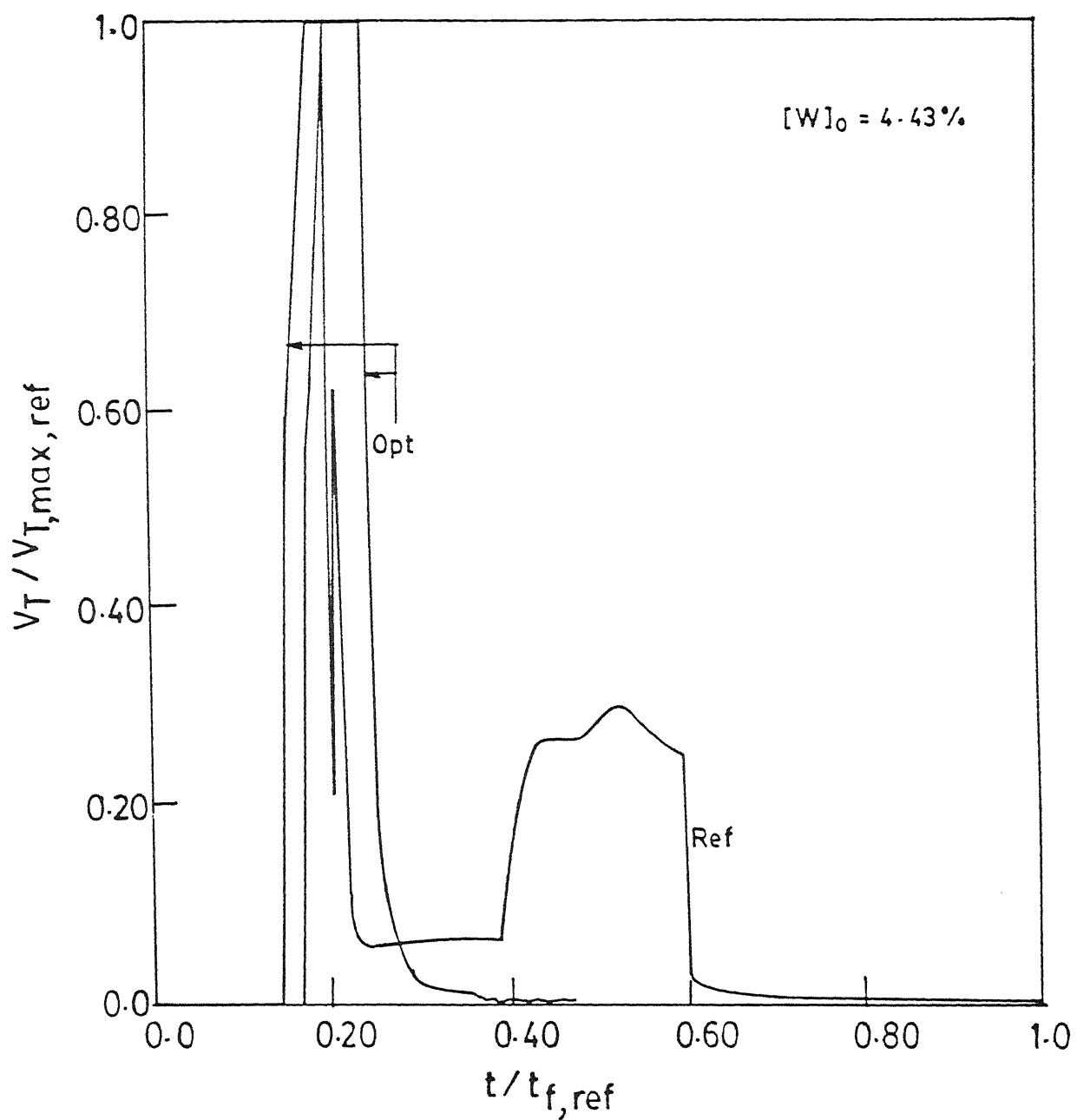


Fig.11 Dimensionless vapor release rate histories. Curve (ref): reference run, (opt): optimal run, for  $T_j = T_{j,ref}$ ,  $[W]_o = 4.43\%$ .

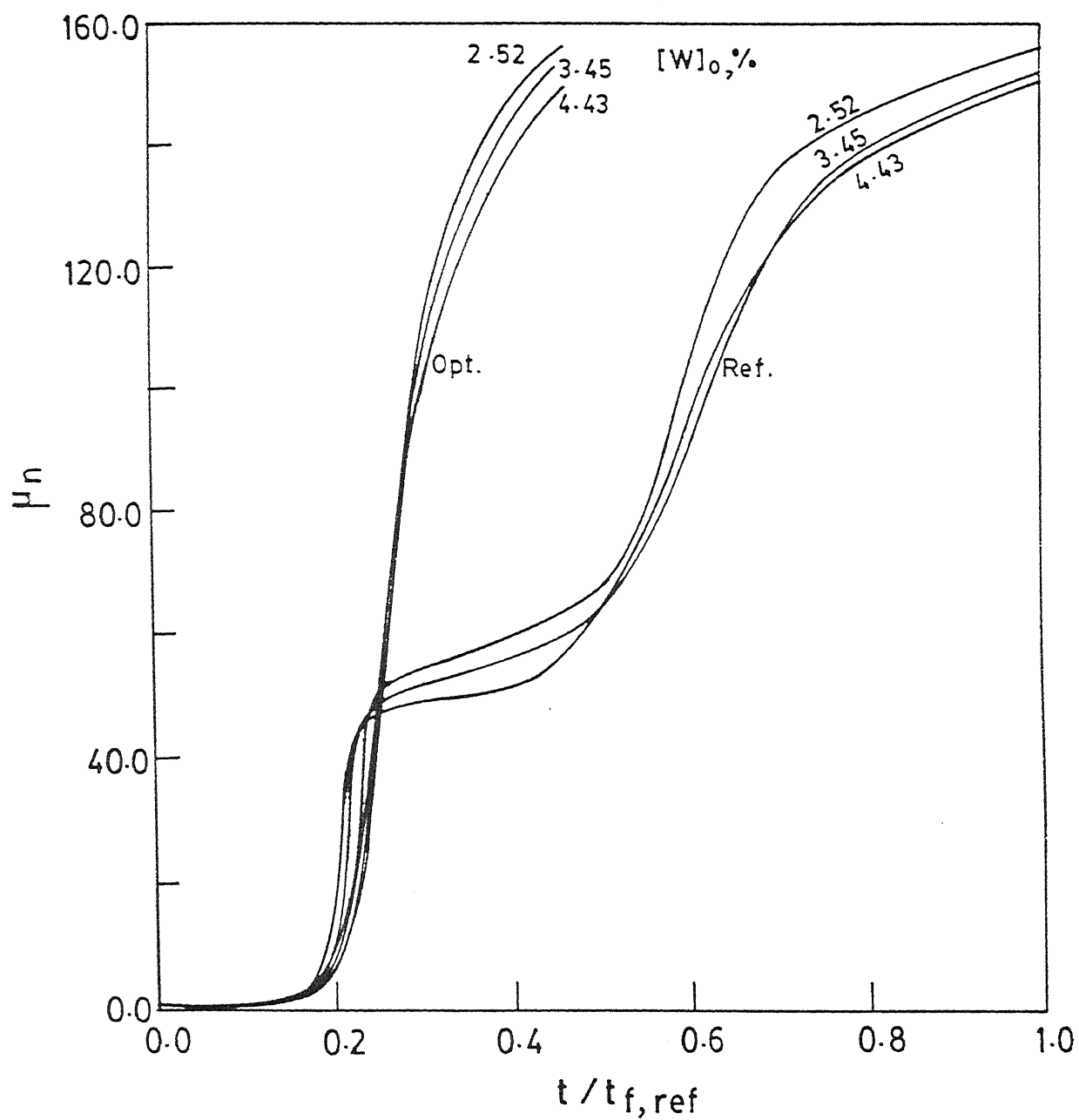


Fig.12 Variation of degree of polymerization with dimensionless time for the reference (ref) and optimal (opt) runs for  $T_j = T_{j,ref}$ ,  $[W]_0 = 2.52\%$ ,  $3.45\%$ ,  $4.43\%$ .

figure it is evident that this plateau does not exist for the optimal histories because of early and rapid pressure decrease, and the  $\mu_n$  increases rapidly at almost a constant rate to the desired value. The value of  $\mu_n$  approaches its final value almost asymptotically at  $t_{f,ref}$  for the reference runs. This is not so for the optimal runs. This makes it necessary to have an excellent control for the reactor so that the value of  $\mu_n$  of the product does not exceed the desired value during emptying of the reactor at the end of the run. With the availability of highly sophisticated and robust controllers, this should not pose any major difficulty.

Fig.13 shows the dimensionless temperature histories for the reference runs as well as for the optimal conditions. In the initial phase, when pressure in the reactor is building up, the temperature variations for the reference runs are similar to those for the optimal runs. This is not surprising since the pressure histories for the optimal and reference runs are quite similar (see Fig.2) in the beginning. However, the temperature histories for the optimal cases deviate from the reference values when the optimal pressure histories start deviating from currently encountered values. This suggests the importance of latent heat effects. Fig.14 shows the variation of monomer conversion with  $t$ , for  $[W]_o=3.45\%$ . It is observed that the conversion rises less sharply for the optimal conditions, than in the reference case. This is attributed to lower temperatures in the optimal case.

Fig.15 shows the variation of the cyclic dimer concentration,  $[C_2]$ , with time. The cyclic dimer concentration remains negligible upto some time and then it starts increasing. The final value for the optimal case are found to be considerably lower than the current values. This is a blessing, since we had obtained the optimal  $V_T(t)$  without putting any requirements on the cyclic dimer concentrations. It must be kept in mind that the low concentration of  $[C_2]_{t_f}$  for optimal runs could increase further during post-polymerization processes (including the emptying of the reactor), since equilibrium is not attained for the reactions involving the

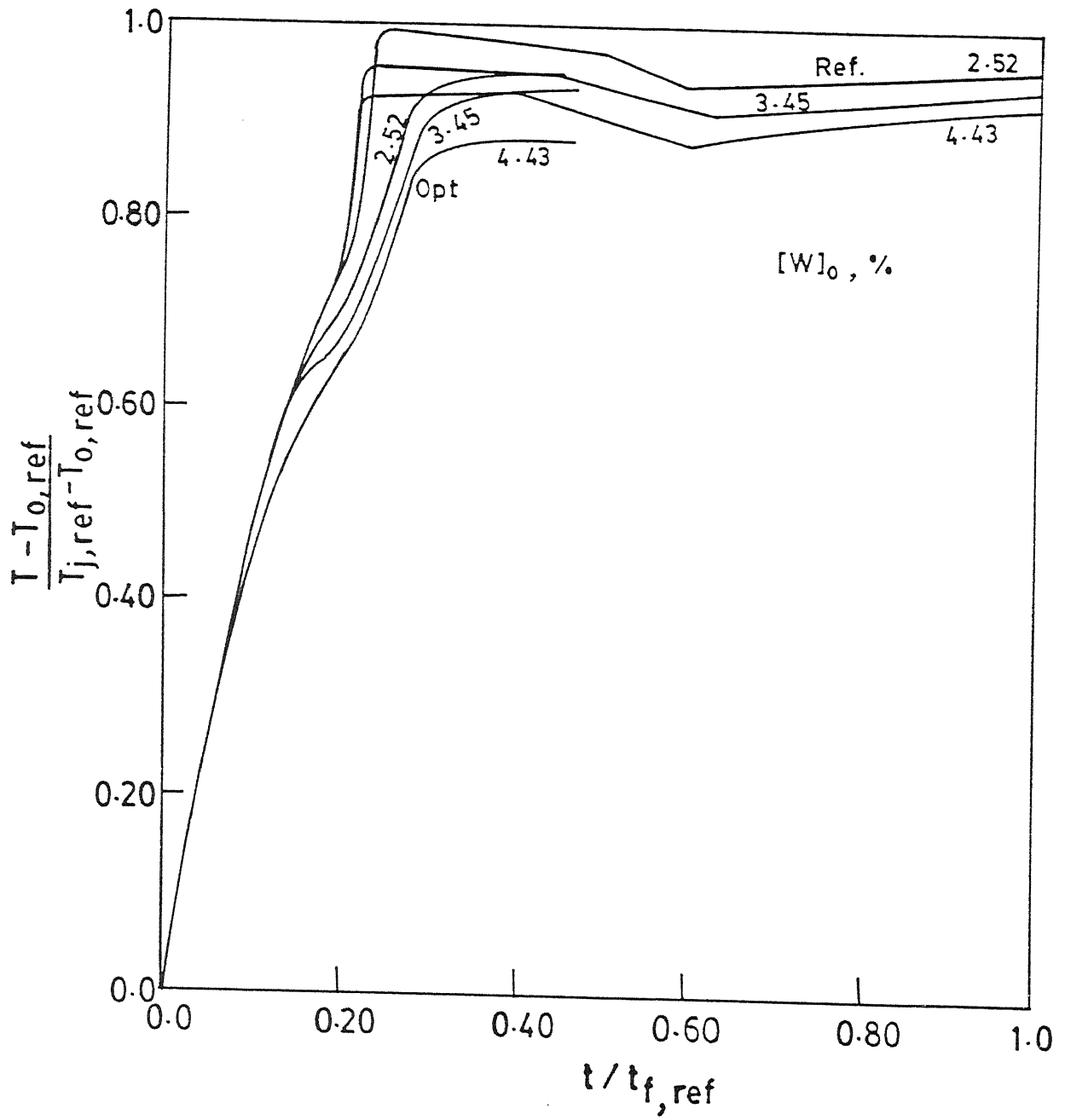


Fig.13 Variation of dimensionless temperature ( $\theta$ ) with dimensionless time for the reference (ref) and optimal (opt) runs for  $T_j = T_{j,ref}$ ,  $[W]_o = 2.52\%$ ,  $3.45\%$ ,  $4.43\%$ .



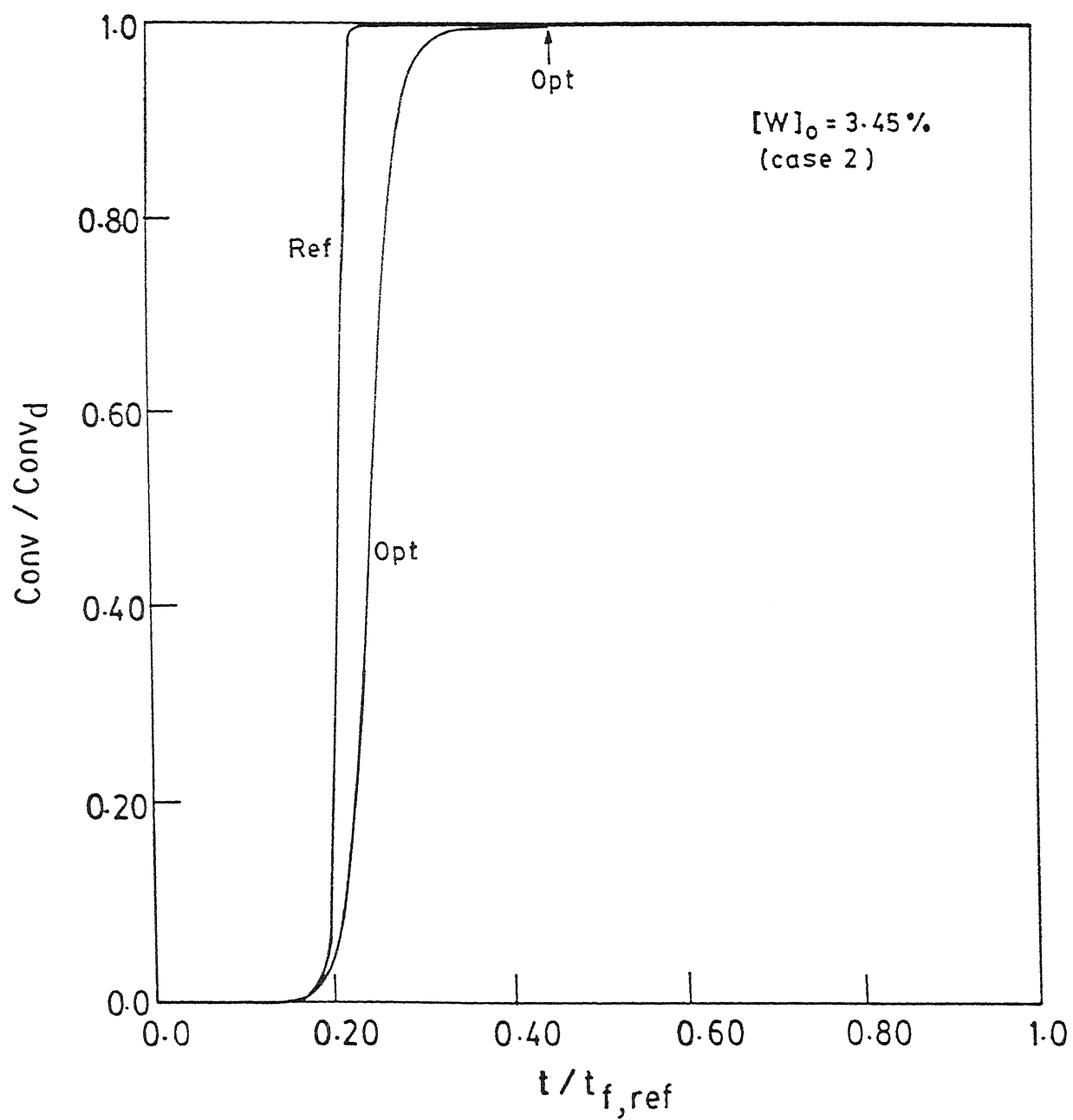


Fig.14 Variation of the dimensionless monomer conversion with dimensionless time for the reference (ref) and optimal (opt) runs for  $T_j = T_{j,ref}$ ,  $[W]_0 = 3.45\%$  (case 2).

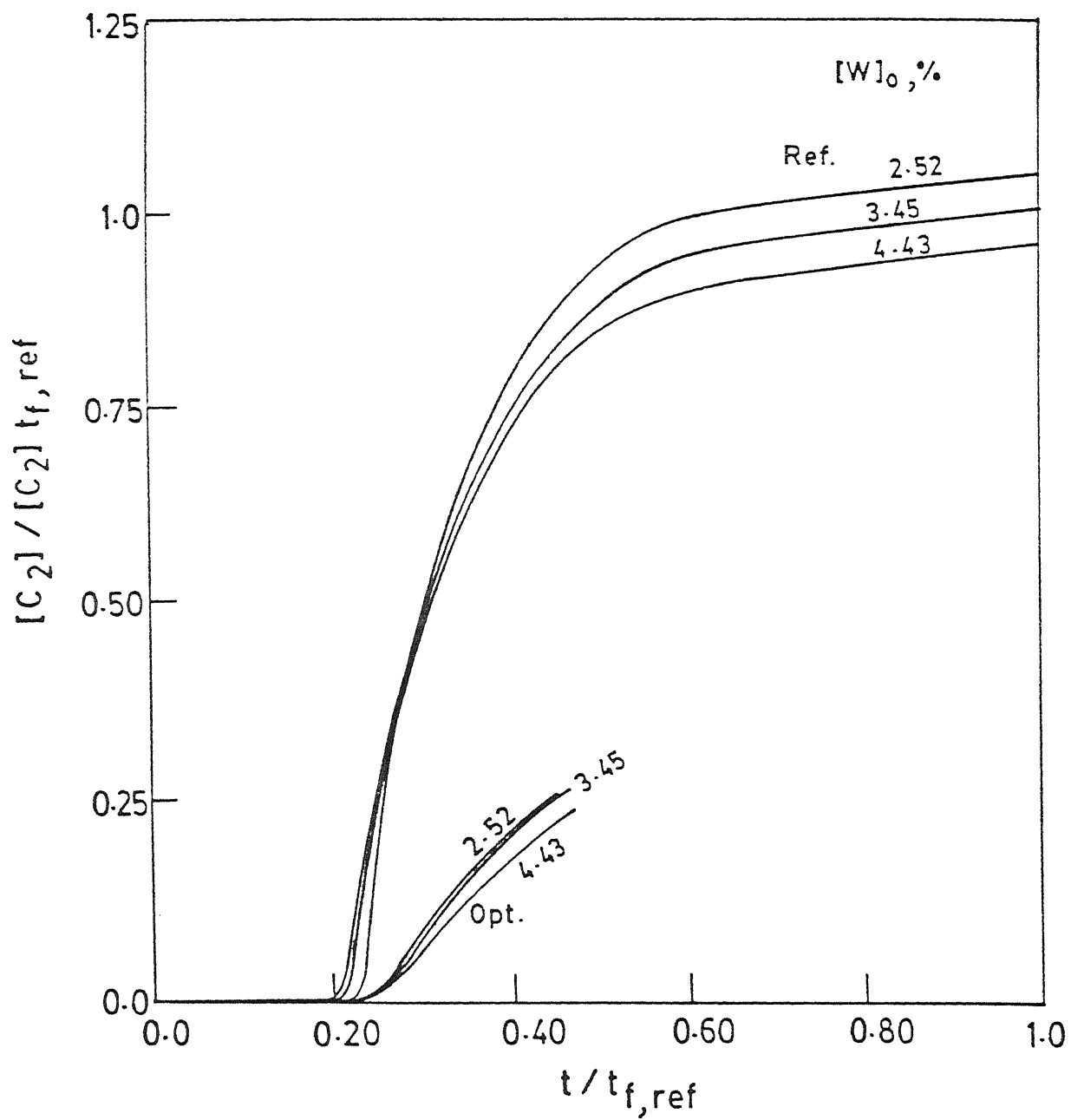


Fig.15 Variation of the dimensionless cyclic dimer concentration with dimensionless time for the reference (ref) and optimal (opt) runs for  $T_j = T_{j,ref}$ ,  $[W]_0 = 2.52\%$ ,  $3.45\%$ ,  $4.43\%$ .

cyclic dimer. However, since one would be ensuring that the values of  $\mu_n$  do not go up beyond the desired values during emptying of the reactor, this requirement should pose no additional problems.

It is interesting to note that the optimal pressure histories obtained (at  $T_j = T_{j,ref}$ ) in the present study using Pontryagin's minimum principle, is quite similar to that obtained by our group earlier [23,24], in which the *shape* of the pressure history was fixed *a priori*, and was determined completely by a few *constants* ( $p_{max}$ ,  $t_c$ ,  $S$ ,  $t_f$ ). Optimal values of three of these constants ( $p_{max}$ ,  $t_c$  and  $S$ , with  $t_f$  determined by the stopping condition of Eq. 6) were determined using sequential quadratic programming. The similarity of the optimal pressure histories as obtained more rigorously in the present study, with the optimal histories obtained with somewhat artificial constraints put on the *shape* of  $p(t)$ , confirms the validity of the constraints used in our earlier study. It may be added that major increases in the plant capacity have been achieved, using some of the results of the present study.

Fig.16 shows how the optimal pressure history changes when the jacket fluid temperature is increased by 5°C. Higher pressures are required (to suppress the vaporization of monomer and water). Use of higher values of  $T_j$  lead to lower values of the objective function. However, it must be ensured that the polymer does not get degraded under these conditions.

In addition to the optimization problem studied above, we also studied the following problem (for  $[W]_o=3.45\%$ )

$$\min I[V_T(t), T_j = T_{j,ref}] \equiv t_f/t_{f,ref} \quad (15)$$

with the following end-point constraint/stopping condition

$$[C_2]_{t_f}/[C_2]_{t_{f,ref}} = 0.2584115 \quad (16)$$

$$\mu_{n,t_f} = 152 \quad (17)$$

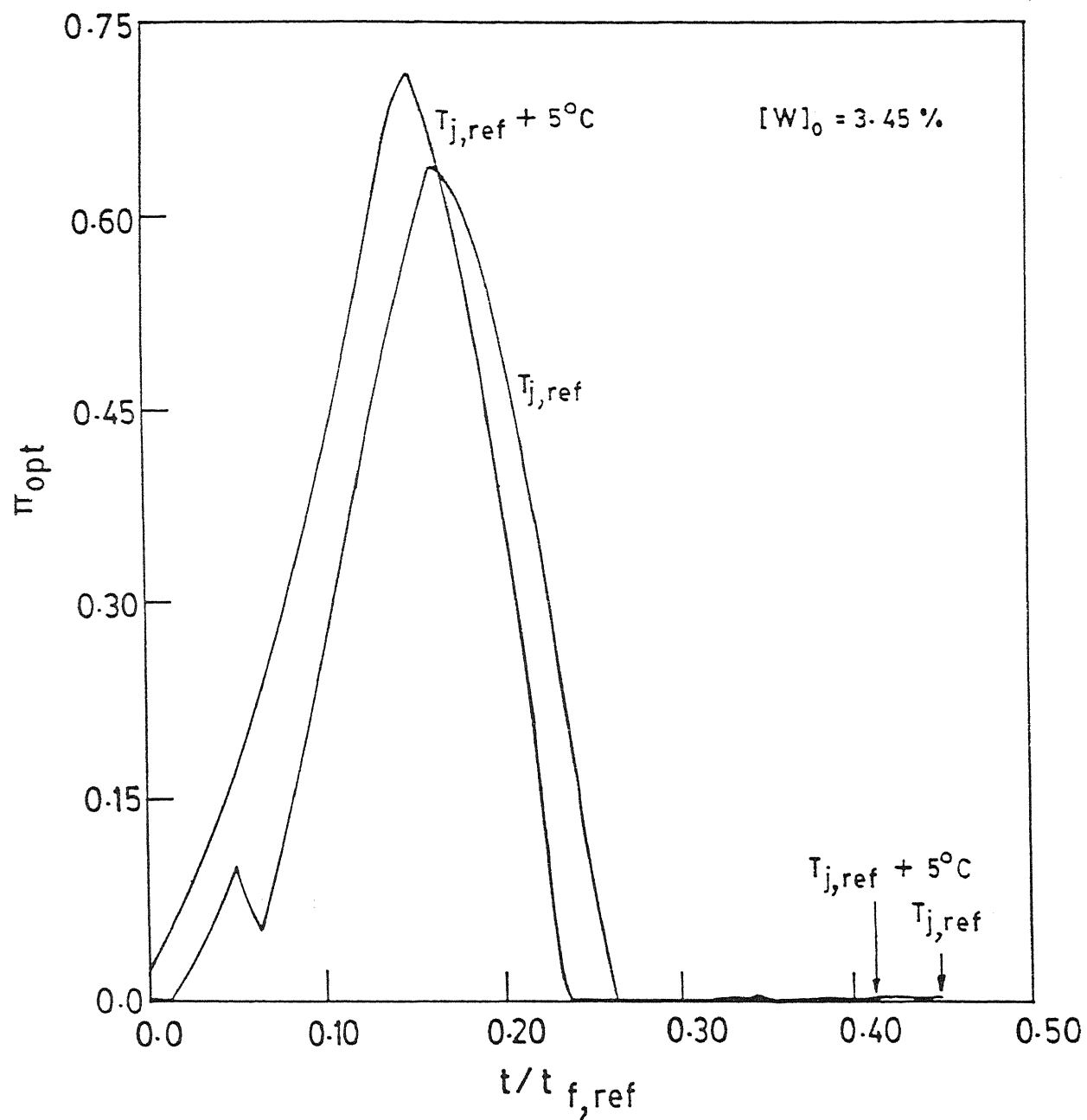


Fig.16 Optimal pressure history using  $T_j = T_{j,ref} + 5^\circ\text{C}$  for the  $[W]_0 = 3.45\%$  case. Optimal history using  $T_j = T_{j,ref}$  also shown for comparison.

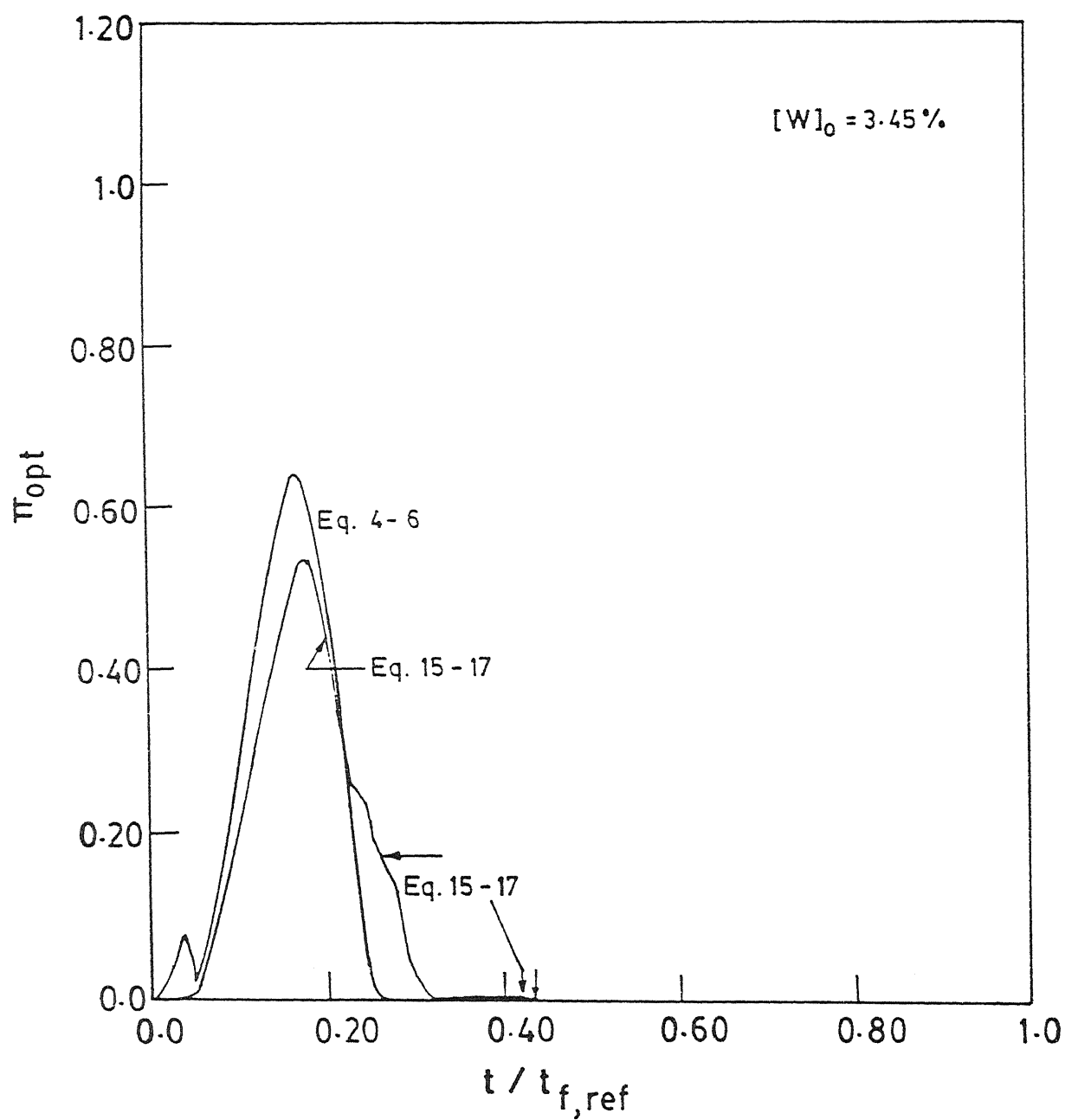


Fig.17 Optimal pressure histories for the two optimization problems described in Eqs. 4-6 and Eqs. 15-17 for  $[W]_0 = 3.45 \%$ .

The values of  $t_f/t_{f,ref}$  and  $conv_{t_f}/conv_d$  under optimal conditions came out as 0.4375 and 0.96689 respectively, which compare very well with the corresponding values of 0.45 and 1.0000 for the problem described in Eqs. 4-6. The optimal pressure histories are shown for the two problems in Fig.17. The results for the two problems seem to be in close agreement and indicate that the optimal results are not affected, significantly, by the type of end-point constraints used.

## CHAPTER 4

# CONCLUSIONS

Optimal vapor release rate histories for an industrial semi-batch nylon 6 reactor, using Pontryagin's minimum principle have been obtained. The results predict a significant reduction in the final reaction time while simultaneously (and somewhat fortuitously) leading to fairly low values of the cyclic dimer concentration in the product. These optimal histories can be implemented on the existing reactor without major alterations and investments. The computational skills developed in this work can also be helpful in the solution of more complicated optimization problems, e.g., multiobjective optimization.

## CHAPTER 5

# SUGGESTIONS FOR FUTURE WORK

Though this work has been able to generate optimal pressure histories which could lead to substantial amount of improvement in the performance of the industrial semi-batch nylon 6 reactor – in terms of total reaction time as well as concentration of undesired cyclic dimer, still it needs to go some steps before it could attain the culmination.

In this study we have assumed that the other manipulated variable i.e. jacket temperature,  $T_j$ , is kept constant throughout the reaction. A more realistic solution of the problem would have been the one in which this variable is included as second control variable. The two control variable problem, which is computationally intensive, was also tried. The convergence was found to be very fast, but the discontinuities in the model did not allow the optimization to proceed after some iterations. Therefore it becomes necessary to remove these discontinuities.

The inclusion of second end-point constraint, dimer concentration  $[C_2]_{t_f}$ , will lead to multiobjective optimization problem. The solution of this problem is called for so that pareto sets are generated to choose the reactor operating conditions as per the need.



## References

- [1] H.K.Reimschuessel, *J. Polym. Sci., Macromol. Revs.*, **12**,65(1977).
- [2] S.K.Gupta and A.Kumar, *Chem. Eng. Commun.*, **20**,1(1983).
- [3] S.K.Gupta and A.Kumar, *Reaction Engineering of Step Growth Polymerization*. Plenum Press, New York,1987.
- [4] K.Tai and T.Tagawa, *Ind. Eng. Chem., Prod. Res. Dev.*, **22**,192(1983).
- [5] S.K.Gupta and A.Kumar, *J. Macromol. Sci., Rev. Macromol. Chem. Phys.*, **C26**.183(1986).
- [6] P.J.Hoftyzer, J.Hoogschagen and D.W. van Krevelen, *Proc. 3rd Eur. Symp. Chem. Rzn. Eng., Amsterdam*, (15-17 Sept.1964), p.247.
- [7] H.K.Reimschuessel and K.Nagasubramanian, *Chem. Eng. Sci.*, **27**,1119(1972).
- [8] K.Nagasubramanian and H.K.Reimschuessel, *J. Appl. Polym. Sci.*, **16**,929(1972).
- [9] W.F.H.Naudin ten Cate, *Proc. Internl. Cong. Use of Elec. Comp. in Chem. Eng.*, Paris, April 1973.
- [10] S.Mochizuki and N. Ito, *Chem. Eng. Sci.*, **33**,1401(1978).
- [11] A.Ramgopal, A.Kumar and S.K.Gupta, *J. Appl. Polym. Sci.*, **28**,2261(1983).
- [12] S.K.Gupta, B.S.Damania and A.Kumar, *J. Appl. Polym. Sci.*, **29**,2177(1984).
- [13] A.K.Ray and S.K.Gupta, *J. Appl. Polym. Sci.*, **30**,4529(1985).
- [14] A.K.Ray and S.K.Gupta, *Polym. Eng. Sci.*, **26**,1033(1986).

- [15] D.Srivastava and S.K.Gupta, *Polym. Eng. Sci.* **31**,596(1991).
- [16] R.M.Wajge and S.K.Gupta, *Polym. Eng. Sci.*, **34**,1161(1994).
- [17] W.H.Ray and J.Szekely, *Process Optimization*, Wiley, New York,1969.
- [18] M.M.Denn, *Optimization by Variational Methods*, McGraw-Hill, New York,1969.
- [19] R.M.Wajge, S.S.Rao and S.K.Gupta, *Polymer*, **35**,3722(1994).
- [20] L.Lapidus and R.Luus, *Optimal Control of Engineering Processes*, Blaisdell, Waltham, MA, 1967.
- [21] A.E.Bryson and Y.C.Ho, *Applied Optimal Control*, Blaisdell, Waltham, MA, 1969.
- [22] S.K.Gupta, *Numerical Methods for Engineers*, New Age International/Wiley Eastern, New Delhi, 1995.
- [23] R.Sareen and S.K.Gupta, *J. Appl. Polym. Sci.*, in press.
- [24] R.Sareen, M.R.Kulkarni and S.K.Gupta, *J. Appl. Polym. Sci.*, **57**,209(1995).

Mass and energy balance equations

$$\begin{aligned}
 \frac{d[C_1]}{dt} &= -k_1[C_1][W] + k'_1[S_1] - k_3[C_1]\mu_o + k'_3(\mu_o - [S_1]) - R_{vm}/F + [C_1] \frac{0.113R_{vm} + 0.018R_{vw}}{F} \\
 \frac{d[S_1]}{dt} &= k_1[C_1][W] - k'_1[S_1] - 2k_2[S_1]\mu_o + 2k'_2[W](\mu_o - [S_1]) - k_3[S_1][C_1] + k'_3[S_2] - k_5[S_1][C_2] + k'_5[S_3] - [S_1] \frac{0.113R_{vm} + 0.018R_{vw}}{F} \\
 \frac{d\mu_o}{dt} &= k_1[C_1][W] - k'_1[S_1] - k_2\mu_o^2 + k'_2[W](\mu_1 - \mu_o) + k_4[W][C_2] - k'_4[S_2] + \mu_o \frac{0.113R_{vm} + 0.018R_{vw}}{F} \\
 \frac{d\mu_1}{dt} &= k_1[C_1][W] - k'_1[S_1] + k_3[C_1]\mu_o - k'_3(\mu_o - [S_1]) + 2k_5[C_2]\mu_o - 2k'_5(\mu_o - [S_1] - [S_2]) + 2k_4[W][C_2] - 2k'_4[S_2] + \mu_1 \frac{0.113R_{vm} + 0.018R_{vw}}{F} \\
 \frac{d\mu_2}{dt} &= k_1[C_1][W] - k'_1[S_1] + 2k_2\mu_1^2 + \frac{1}{3}k'_2[W](\mu_1 - \mu_3) + k_3[C_1](\mu_o + 2\mu_1) + k'_3(\mu_o - 2\mu_1 + [S_1]) + 4k_5[C_2](\mu_o - \mu_1) + 4k'_5(\mu_o - \mu_1 + [S_2]) \\
 &\quad + 4k_4[W][C_2] - 4k'_4[S_2] + \mu_2 \frac{0.113R_{vm} + 0.018R_{vw}}{F} \\
 \frac{d[C_2]}{dt} &= -k_4[C_2][W] + k'_4[S_2] - k_5[C_2]\mu_o + k'_5(\mu_o - [S_1] - [S_2]) + [C_2] \frac{0.113R_{vm} + 0.018R_{vw}}{F} \\
 \frac{d[W]}{dt} &= -k_1[C_1][W] + k'_1[S_1] + k_2\mu_o^2 - k'_2[W](\mu_1 - \mu_o) - k_4[C_2][W] + k'_4[S_2] - R_{vw}/F + [W] \frac{0.113R_{vm} + 0.018R_{vw}}{F} \\
 \frac{dF}{dt} &= -(0.113R_{vm} + 0.018R_{vw}) \\
 \frac{dT}{dt} &= \left\{ UA(T_j - T) + \frac{F}{1000} \sum_{i=1}^5 r_i(-\Delta H_i) - [R_{vm}\lambda_m(T) + R_{vw}\lambda_w(T)] - [0.113R_{vm}C_{p,m} + 0.018R_{vw}C_{p,w}](T - T_i) + C_{p,mix}[0.113R_{vm} + 0.018R_{vw}](T - T_i) \right\} \\
 &\quad \times \{ [C_{p,mix} + 2.0925 \times 10^{-3}(T - T_i)]F \}^{-1} \\
 \frac{d[M^*]}{dt} &= \frac{R_{vm}}{V_g} - \frac{V_T[M^*]}{V_g([M^*] + [W^*] + [N^*])} \\
 \frac{d[W^*]}{dt} &= \frac{R_{vw}}{V_g} - \frac{V_T[W^*]}{V_g([M^*] + [W^*] + [N^*])} \\
 \frac{d[N^*]}{dt} &= -\frac{V_T[N^*]}{V_g([M^*] + [W^*] + [N^*])} \\
 \frac{d\check{s}_1}{dt} &= R_{vm} \\
 \frac{d\check{s}_2}{dt} &= R_{vw} \\
 \frac{d\check{s}_3}{dt} &= V_T \\
 \text{Closure conditions:} \\
 [S_3] &= [S_2] = [S_1] \\
 \mu_3 &= \frac{\mu_2(2\mu_2\mu_o - \mu_1^2)}{\mu_1\mu_o}
 \end{aligned}$$

Expression for  $V_T$ Stage 1:  $V_T = 0$ 

$$\text{Stages 2-5: } V_T = R_{vm} + R_{vw} - \frac{V_g}{RT} \left( \frac{dP}{dt} \right) + V_g \frac{[M^*] + [W^*] + [N^*]}{T} \left( \frac{dT}{dt} \right)$$

Rates of vaporization

$$R_{vm} = F(k_{1,m}a)_f([C_1] - [C_1]^*) \quad [C_1]^* = \frac{[W] - [C_1]}{\gamma_m P_m^{sat}} [M^*] RT$$

$$R_{vw} = F(k_{1,w}a)_f([W] - [W]^*) + F(k_{1,w}a)_b([W] - [W]^*)$$

$$[W]^* = \frac{[W] + [C_1]}{\gamma_w P_w^{sat}} [W^*] RT \quad [W]^* = \frac{[C_1](P - P_m^{sat})}{(\gamma_w P_w^{sat} - P)}$$

Pressure

$$P = ([M^*] + [W^*] + [N^*]) RT$$

Equations for activity coefficients

$$\text{monomer conversion} = 1.0 - \frac{F[C_1]}{F_0[C_1]_0 - \dot{V}_1}$$

$$\gamma_m = \beta_{m0} + \frac{\beta_{m1} - \beta_{m0}}{0.95} (\text{monomer conversion})$$

$$\gamma_w = \beta_{w0} + \frac{\beta_{w1} - \beta_{w0}}{0.95} (\text{monomer conversion})$$

Vapour pressure

$$\ln[P_m^{sat} (\text{kPa}) / 101.3] = 13.0063 - \frac{7024.023}{T(K)} \quad (\text{ref. 16})$$

$$\ln[P_w^{sat} (\text{kPa}) / 101.3] = 11.6703 - \frac{3816.44}{T(K) - 46.13} \quad (\text{ref. 17})$$

Diffusion coefficients

$$\mathcal{D}_w (\text{m}^2 \text{h}^{-1}) = 3.6 \times 10^{-6}$$

$$\mathcal{D}_m (\text{m}^2 \text{h}^{-1}) = 2.88 \times 10^{-8}$$

Latent heats of vaporization

$$T_r = 473.15 \text{ K}$$

$$\lambda_w(T_r) = 34.2559 \text{ kJ mol}^{-1} \quad (\text{ref. 18})$$

$$\lambda_m(T_r) = 51.0193 \text{ kJ mol}^{-1} \quad (\text{ref. 18})$$

$$C_{p,m}^\circ = 1.6426 \text{ kJ kg}^{-1} \text{K}^{-1} \quad (\text{ref. 18})$$

$$C_{p,w}^\circ = 1.9963 \text{ kJ kg}^{-1} \text{K}^{-1} \quad (\text{ref. 18})$$

Heat transfer coefficient

$$h_i (\text{kJ h}^{-1} \text{m}^{-2} \text{K}^{-1}) = \frac{h_{ref}}{[\eta (\text{Pa s})]^{0.17}}$$

$$U = \frac{1}{\frac{1}{h_i} + \frac{\text{thickness (m)}}{k_{ss}}}$$

Correlations from ref. 19 for mixture physical properties (liquid)

$$C_{p,mix}^\circ (\text{kJ kg}^{-1} \text{K}^{-1}) = 2.0925 + 2.0925 \times 10^{-3} [T(K) - 273.15]$$

$$\rho (\text{kg m}^{-3}) = 1000[1.1238 - 0.5663 \times 10^{-3} [T(K) - 273.15]]$$

$$k (\text{kJ h}^{-1} \text{m}^{-1} \text{K}^{-1}) = 0.7558$$

Correlations from ref. 20 for mass transfer coefficients

$$N_{Re} = \frac{d_i^2 n \rho}{6 \eta (\text{poise})}$$

$$N_{Sc,i} = \frac{360 \eta (\text{poise})}{\rho \mathcal{D}_i}$$

$$\Omega_b = \left( \frac{[C_1]}{[C_1] + [W]} \gamma_m P_m^{sat} + \frac{[W]}{[C_1] - [W]} \gamma_w P_w^{sat} \right)$$

(i) Quiescent (q) desorption ( $\Omega_b < P$ )

$$N_{Sh,i,q} = 0.322 N_{Re}^{0.7} N_{Sc,i}^{0.33} \quad i = m \text{ or } w$$

$$N_{Sh,i,q} = \frac{(k_{1,i})_{f,q} D_i}{\mathcal{D}_i}$$

$$a_{f,q} = \frac{(\pi/4) D_i^2}{(F/\rho)}$$

$$(k_{1,m}a)_f = (k_{1,m}a)_{f,q}$$

$$(k_{1,w}a)_f = (k_{1,w}a)_{f,q}$$

$$(k_{1,w}a)_b = 0$$

(ii) Bubbly (b) desorption ( $\Omega_b > P$ )

$$\sigma = \frac{[W] - [W_b]^*}{[W_b]^*}$$

$$\sigma_c = 1.81 N_{Re}^{-0.25}$$

If  $\sigma < \sigma_c$ :

$$(k_{1,w}a)_b (\text{h}^{-1}) = 6.77 \times 10^{-6} N_{Re}^{0.5} \sigma^{0.78} \times 3600$$

$$(k_{1,m}a)_f = (k_{1,m}a)_{f,q}$$

$$(k_{1,w}a)_f = (k_{1,w}a)_{f,q}$$

If  $\sigma > \sigma_c$ :

$$(k_{1,w}a)_b (\text{h}^{-1}) = 2.45 \times 10^{-6} N_{Re}^{0.3} \sigma^{0.5} \times 3600$$

$$\log_{10} \phi = 522(\sigma - \sigma_c) N_{Re}^{-0.81}$$

$$(k_{1,m}a)_f = (k_{1,m}a)_{f,q} \phi$$

$$(k_{1,w}a)_f = (k_{1,w}a)_{f,q} \phi$$

Viscosity correlation (neglecting effect of water)

$$\eta_m (\text{cp}) = 2.7969 \times 10^{-4} \exp[3636.364/T(K)] \quad \text{for } T > 473.15 \text{ K}$$

$$[\eta] \left( \frac{100 \text{ kg mixture}}{\text{kg polymer}} \right) = \lim_{c \rightarrow 0} \frac{\eta_{sp}}{c} = \lim_{c \rightarrow 0} \frac{\eta - \eta_m}{\eta_m} \frac{1}{c} = \left[ -\frac{1875.0}{T(K)} + 4.678 \right] \left( \frac{M_n}{5424} \right)^{0.75}$$

$$M_n = 113 \mu_1 / \mu_0 \quad M_w = 113 \mu_2 / \mu_1$$

$$c (\text{kg polymer}/100 \text{ kg mixture}) = 11.3 \mu_1$$

For  $c < 21.0/[\eta]$ 

$$\frac{\eta_{sp}}{c[\eta]} = 1.0 - 0.3102c[\eta] + 0.0575(c[\eta])^2 - 0.525 \times 10^{-2}(c[\eta])^3 + 0.2305 \times 10^{-3}(c[\eta])^4 - 0.3663 \times 10^{-5}(c[\eta])^5$$

For  $c > 21.0/[\eta]$ 

$$\log_{10} \eta (\text{poise}) = 5 \log_{10}(C_s^* M_w^{0.68}) - 12.3097$$

$$\text{for } C_s^* M_w^{0.68} > 315 \text{ and } M_w > 5000$$

else

$$\log_{10} \eta (\text{poise}) = \log_{10}(C_s^* M_w) - 3.503$$

$$\text{where } C_s^* (\text{g polymer}/\text{cm}^3 \text{ mixture}) = 11.3 \times 10^{-5} \rho \mu_1$$

Appendix 2  
EQUATIONS FOR OPTIMALITY WITH END POINT CONSTRAINTS AND  
STOPPING CONDITIONS

1. Objective Function

$$\min \mathbf{I}[\mathbf{x}(t_f), t_f]$$

2. Mass Balance (State Variable) Equations

$$\frac{d\mathbf{x}}{dt} \equiv \begin{bmatrix} \frac{dx_1}{dt} \\ \frac{dx_2}{dt} \\ \vdots \\ \frac{dx_n}{dt} \end{bmatrix} = \mathbf{f}[\mathbf{x}(t), \mathbf{u}(t)] = \begin{bmatrix} f_1(\bar{x}, \bar{u}) \\ f_2(\bar{x}, \bar{u}) \\ \vdots \\ f_n(\bar{x}, \bar{u}) \end{bmatrix}$$

with

$$\mathbf{u}^T(t) \equiv [u_1, u_2, \dots, u_l]$$

3. End Point Constraints

$$\Psi[\mathbf{x}(t_f), t_f] \equiv \begin{bmatrix} \psi_1(\mathbf{x}(t_f), t_f) \\ \psi_2(\mathbf{x}(t_f), t_f) \\ \vdots \\ \psi_m(\mathbf{x}(t_f), t_f) \end{bmatrix} = \mathbf{0}$$

4. Stopping Conditions

$$\rho[\mathbf{x}(t_f), t_f] \equiv \rho[x_1(t_f), x_2(t_f), \dots, x_n(t_f); t_f] = 0$$

5. Constraints on Control Variable  $\mathbf{u}$

$$\mathbf{u}_{min} \leq \mathbf{u} \leq \mathbf{u}_{max}$$

6. Adjoint Function Equations

(a)

$$\frac{d\lambda^I(t)}{dt} = \frac{d}{dt} \begin{bmatrix} \lambda_1^I \\ \lambda_2^I \\ \vdots \\ \lambda_n^I \end{bmatrix} \equiv -\mathbf{A}^T(t)\lambda^I(t); \lambda^I(t_f) = \left( \frac{\partial \mathbf{I}}{\partial \mathbf{x}} \right)_{t=t_f}$$

where

$$\mathbf{A}^T(t) = \frac{\partial \mathbf{f}^T}{\partial \mathbf{x}} \equiv \begin{bmatrix} \frac{\partial f_1}{\partial x_1} \frac{\partial f_2}{\partial x_1} \dots \frac{\partial f_n}{\partial x_1} \\ \frac{\partial f_1}{\partial x_2} \frac{\partial f_2}{\partial x_2} \dots \frac{\partial f_n}{\partial x_2} \\ \vdots \\ \frac{\partial f_1}{\partial x_n} \frac{\partial f_2}{\partial x_n} \dots \frac{\partial f_n}{\partial x_n} \end{bmatrix}$$

(b)

$$\frac{d\lambda^\Psi(t)}{dt} \equiv \frac{d}{dt} \begin{bmatrix} \lambda_1^{\psi_1} \lambda_1^{\psi_2} \dots \lambda_1^{\psi_m} \\ \lambda_2^{\psi_1} \lambda_2^{\psi_2} \dots \lambda_1^{\psi_m} \\ \vdots \\ \lambda_n^{\psi_1} \lambda_n^{\psi_2} \dots \lambda_n^{\psi_m} \end{bmatrix} = -\mathbf{A}^T(t) \lambda^\Psi(t); \lambda^\Psi(t_f) = \left( \frac{\partial \Psi^T}{\partial \mathbf{x}} \right)_{t=t_f}$$

(c)

$$\frac{d\lambda^\rho(t)}{dt} = \frac{d}{dt} \begin{bmatrix} \lambda_1^\rho \\ \lambda_2^\rho \\ \vdots \\ \lambda_n^\rho \end{bmatrix} = -\mathbf{A}^T(t) \lambda^\rho(t); \lambda^\rho(t_f) = \left( \frac{\partial \rho}{\partial \mathbf{x}} \right)_{t=t_f}$$

### 7. Increment In $\mathbf{u}(t)$

$$\begin{aligned} \partial \mathbf{u}(t)_{(1 \times 1)} &= -\mathbf{B}_{(1 \times n)}^T(t) \left[ \lambda_{(n \times 1)}^{\mathbf{I}\rho}(t) - \lambda_{(n \times m)}^{\Psi\rho}(t) \mathbf{I}_{\Psi\Psi(m \times m)}^{-1} \mathbf{I}_{\Psi\mathbf{I}(m \times 1)} \right] \times \\ &\quad \left[ \frac{r^2 - \partial \Psi_{(1 \times m)}^T \mathbf{I}_{\Psi\Psi(m \times m)}^{-1} \partial \Psi_{(m \times 1)}}{\mathbf{I}_{II(1 \times 1)} - \mathbf{I}_{\Psi\Psi(m \times m)}^{-1} \mathbf{I}_{\Psi\mathbf{I}(m \times 1)}} \right]^{\frac{1}{2}} + \\ &\quad \mathbf{B}_{(1 \times n)}^T(t) \lambda_{(n \times m)}^{\Psi\rho}(t) \mathbf{I}_{\Psi\Psi(m \times m)}^{-1} \partial \Psi_{(m \times 1)} \end{aligned}$$

where

$$\mathbf{I}_{\Psi\Psi(m \times m)} = \int_0^{t_f} \left( \lambda_{(m \times n)}^{\Psi\rho}(t) \right)^T \mathbf{B}_{(n \times 1)}(t) \mathbf{B}_{(1 \times n)}^T(t) \lambda_{(n \times 1)}^{\Psi\rho}(t) dt$$

$$\mathbf{I}_{\Psi\mathbf{I}(m \times 1)} = \int_0^{t_f} \left( \lambda_{(m \times n)}^{\Psi\rho}(t) \right)^T \mathbf{B}_{(n \times 1)}(t) \mathbf{B}_{(1 \times n)}^T(t) \lambda_{(n \times 1)}^{\mathbf{I}\rho}(t) dt$$

$$\mathbf{I}_{II(1 \times 1)} = \int_0^{t_f} \left( \lambda_{(1 \times n)}^{\mathbf{I}\rho}(t) \right)^T \mathbf{B}_{(n \times 1)}(t) \mathbf{B}_{(1 \times n)}^T(t) \lambda_{(n \times 1)}^{\mathbf{I}\rho}(t) dt$$

$$\lambda_{(n \times 1)}^{\mathbf{I}\rho}(t) = \lambda_{(n \times 1)}^{\mathbf{I}}(t) - \lambda_{(n \times 1)}^\rho(t) \left[ \frac{\frac{\partial \mathbf{I}}{\partial t} + \left( \frac{\partial \mathbf{I}}{\partial \mathbf{x}} \right)^T \mathbf{f}}{\frac{\partial \rho}{\partial t} + \left( \frac{\partial \rho}{\partial \mathbf{x}} \right)^T \mathbf{f}} \right]_{t=t_f}$$

$$\lambda_{(n \times m)}^{\Psi \rho}(t) = \lambda_{(n \times m)}^{\Psi}(t) - \lambda_{(n \times 1)}^{\rho}(t) \left[ \frac{\left[ \frac{\partial \Psi}{\partial t} + \left( \frac{\partial \Psi^T}{\partial t} \right) \mathbf{f} \right]_{1 \times m}^T}{\frac{\partial \rho}{\partial t} + \left( \frac{\partial \rho}{\partial t} \right)^T \mathbf{f}} \right]_{t=t_f}$$

$$\mathbf{B}_{l \times n}^T = \left( \frac{\partial \mathbf{f}^T}{\partial \mathbf{u}} \right) \equiv \begin{bmatrix} \frac{\partial f_1}{\partial u_1} \frac{\partial f_2}{\partial u_1} \dots \frac{\partial f_n}{\partial u_1} \\ \frac{\partial f_1}{\partial u_2} \frac{\partial f_2}{\partial u_2} \dots \frac{\partial f_n}{\partial u_2} \\ \vdots \\ \frac{\partial f_1}{\partial u_l} \frac{\partial f_2}{\partial u_l} \dots \frac{\partial f_n}{\partial u_l} \end{bmatrix}_{(l \times n)}$$

## 8. Increment $\delta \Psi$

$$\delta \Psi_{(m \times 1)} = -\varepsilon^* \Psi(t_f); 0 \leq \varepsilon \leq 1$$